Accepted Manuscript

Targeting tubulin polymerization by novel 7-aryl-pyrroloquinolinones: Synthesis, biological activity and SARs

Roberta Bortolozzi, Elena Mattiuzzo, Matteo Dal Pra, Mattia Sturlese, Stefano Moro, Ernest Hamel, Davide Carta, Giampietro Viola, Maria Grazia Ferlin

PII: S0223-5234(17)30941-8

DOI: 10.1016/j.ejmech.2017.11.038

Reference: EJMECH 9913

To appear in: *European Journal of Medicinal Chemistry*

Received Date: 6 October 2017

Revised Date: 15 November 2017

Accepted Date: 17 November 2017

Please cite this article as: R. Bortolozzi, E. Mattiuzzo, M.D. Pra, M. Sturlese, S. Moro, E. Hamel, D. Carta, G. Viola, M.G. Ferlin, Targeting tubulin polymerization by novel 7-aryl-pyrroloquinolinones: Synthesis, biological activity and SARs, *European Journal of Medicinal Chemistry* (2017), doi: 10.1016/j.ejmech.2017.11.038.

Targeting tubulin polymerization by novel 7-aryl-pyrroloquinolinones: synthesis, biological activity and SARs.

Roberta Bortolozzi[1*], Elena Mattiuzzo[1*], Matteo Dal Pra[2], Mattia Sturlese[2], Stefano Moro[2], Ernest Hamel[3], Davide Carta[2], Giampietro Viola[1], Maria Grazia Ferlin[2]

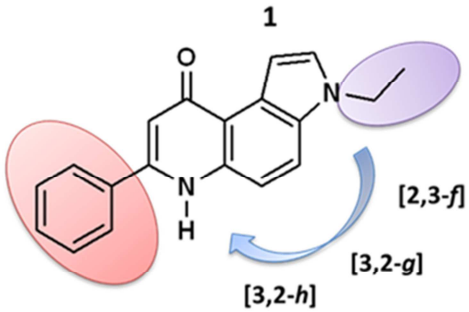

The three main structural determinants for potent cytotoxicity (GI_{50} = 0.2-123 nM) modified for obtaining novel PyQs were the 3- and 7-substituents and the angular geometries.

Targeting tubulin polymerization by novel 7-aryl-pyrroloquinolinones: synthesis, biological activity and SARs.

Roberta Bortolozzi[1*], Elena Mattiuzzo[1*], Matteo Dal Pra[2], Mattia Sturlese[2], Stefano Moro[2], Ernest Hamel[3], Davide Carta[2], Giampietro Viola[1], Maria Grazia Ferlin[2]

[1]*Department of Woman's and Child's Health, University of Padova, Laboratory of Oncohematology, 35128 Padova, Italy.*

[2]*Department of Pharmaceutical and Pharmacological Sciences, University of Padova, 35131 Padova, Italy.*

[3]*Screening Technologies Branch, Developmental Therapeutics Program, Division of Cancer Treatment and Diagnosis, Frederick National Laboratory for Cancer Research, National Cancer Institute, National Institutes of Health, Frederick, Maryland 21702, USA.*

*equal contributing authors

Abstract

Earlier studies had confirmed that the 7-phenylpyrroloquinolinone (7-PPyQ) nucleus was an important scaffold for new chemotherapeutic drugs targeting microtubules. For wide-ranging SARs, a series of derivatives were synthesized through a robust procedure. For comparison with the reference 3-ethyl-7-PPyQ **31**, the angular geometry and substituents at the 3 and 7 positions were varied to explore interactions inside the colchicine site of tubulin. Of the new compounds synthesized, potent cytotoxicity (low and sub-nanomolar GI_{50} values) was observed with **21** and **24**, both more potent than **31,** in both leukemic and solid tumor cell lines. Neither compound **21** nor **24** induced significant cell death in normal human lymphocytes, suggesting that the compounds may be selectively active against cancer cells. In particular, **24** was a potent inducer of apoptosis in the A549 and HeLa cell lines. With both compounds, induction of apoptosis was associated with dissipation of the mitochondrial transmembrane potential and production of reactive oxygen species, indicating that cells treated with the compounds followed the intrinsic pathway of apoptosis. Moreover, immunoblot analysis revealed that compound **24** even at 50 nM reduced the expression of anti-apoptotic proteins such as Bcl-2 and Mcl-1. Finally, molecular docking studies of the newly synthesized compounds demonstrate that active pyrroloquinolinone derivatives strongly bind in the colchicine site of β-tubulin.

Keywords. Microtubules, phenylpyrroloquinolinone, tubulin, apoptosis, molecular docking, structure-activity relationships.

1. Introduction

A major difference between cancer cells and many healthy cells is that transformed cells often divide much faster. The microtubule (MT) cytoskeleton is highly dynamic in mitosis, and therefore dividing cells are particularly susceptible to agents that target tubulin [1]. Colchicine site inhibitors exert their biological effects by inhibiting tubulin assembly and suppressing microtubule formation [2]. Despite significant structural diversity, colchicine site inhibitors are believed to act by a common mechanism via binding to the colchicine site on tubulin. Among them, we can include 7-phenyl-pyrroloquinolinones (7-PPyQs) and, especially, the 3-substituted derivatives bind to the site with high affinity, inhibiting microtubule assembly and therefore producing a strong antiproliferative effect. Their activities are similar to those of the reference compound combretastatin A-4 [3-9]. The more cytotoxic 7-PPyQ derivatives showed remarkably *in vitro* biological properties and good antitumor activity *in vivo* [3]. Some 7-PPyQs, characterized by alkyl substituents at the pyrrole nitrogen, show increased cytotoxicity with nanomolar and sub-nanomolar GI_{50} values and overcome the resistance observed with the clinically used drugs vincristine and taxol [4].In an effort to produce additional highly active compounds, numerous related analogs were designed, synthesized and studied, resulting in the discovery of potent 3*N*-acyl derivatives showing low nanomolar GI_{50} values and an anti-tubulin mechanism profile similar to that previously observed [8]. Moreover, the most recent 3-benzoyl-7-PPyQ is even more cytotoxic than the initially reported compounds. Moreover, the 3-benzoyl-7-PPyQ has minimal toxicity for nontumor cell lines, good in vitro metabolic stability and synergizes with conventional chemotherapeutic agents in inhibiting leukemia cell proliferation [9]. Through a tubulin docking study with 7-PPyQ amide derivatives at the colchicine site, we observed a hydrogen bond involving the 6-NH and strong hydrophobic interactions due to the pyrrolo[3,2-*f*]quinolinone scaffold and to the phenyl ring at position 7. The substituents at the 3*N*-pyrrole were placed in a pocket formed by numerous amino

acid residues. This binding mode is compatible with a competitive mechanism of action at the colchicine site.

In the present study, we enrich the available library of pyrroloquinolinone derivatives to obtain greater knowledge of SARs for further development of PPyQs and to understand better how PPyQs are accommodated in the colchicine site pocket.

The reference compound, 3-ethyl-7-phenyl-3*H*-pyrrolo[3-2-*f*]quinolin-9-one (**31**, Figure 1) was our start point for chemical modifications [4]. Compound **31** has the elements determined to be crucial for anti-tubulin activity, such as the [3,2-*f*] configuration, the 7-phenyl and 9-carbonyl groups and the ethyl group at position 3. All these elements were important for good antiproliferative effects. This study explores the role of larger 3 and 7 substituents and various scaffold geometries. Among our most interesting findings were that placement of a naphthalene moiety at the 7 position, a 3N-*n*-octadecyl alkyl chain and [3,2-*g*] and [3,2-*h*] geometries led to enhanced cytotoxicity. The synthesis and biological activities of the new compounds are summarized in this report.

2. Results and discussion

2.1 Chemistry

The 4-step method leading to 7-PPyQ compounds was previously described [4] (Scheme 1). First, commercially available 5-, 6- or 7-nitroindoles were subjected to an *N*-alkylation reaction using appropriate halogenated compounds to obtain the nitroindole derivatives **1-4**. The same reaction conditions were used with the chloro- and bromo-compounds in anhydrous DMF in the presence of NaH, at room temperature with the ethyl bromide and 50° C with the *n*-octadecyl chloride, resulting in high yields of the reaction products. The catalytic reduction (Pd/C 10%, H_2 at atmospheric pressure, ethyl acetate) of intermediates **1-4** gave the corresponding aminoindoles **5-8** in almost quantitative yields. The non-commercially available β-ketoesters **9-12** were prepared following a method reported in the literature [10] by reacting the appropriate methyl-aryl ketone and diethyl

carbonate in the presence of NaH, in anhydrous dioxane at 80° C for 6 h, with good yields. Next, in order to obtain the enamine derivatives **13-18** as condensation products of the reactions between the *β*-ketoesters and aminoindoles**,** compounds **5** and **6** were reacted with commercial ethyl acetoacetate, benzoyl acetate and the prepared compounds **9-12**. All the reactions were carried out in absolute ethanol at reflux in the presence of a catalytic amount of acetic acid, yielding the acrylate derivatives as crude material **13-18**. These had to be purified by silica gel column chromatography before being submitted to thermal cyclization in boiling diphenyl ether (250 °C) to obtain the final products **19-24**. Using the same reaction conditions, enamines **25** and **28** were also obtained by reacting 3-ethyl-6-aminoindole (**7**) and 3-ethyl-7-amino-indole (**8**) with benzoyl acetate. These compounds were also purified before being cyclized to the tricyclic products. In the case of enamine **25**, an un-resolvable mixture of two cyclized compounds was obtained**.** By NMR spectroscopy it was possible to identify compound **26** as a [2,3-*f*] angular and **27** as a [3,2-*g*] linear PPyQ. In the same way, from enamine **28** a mixture was obtained that was separated giving the two compounds in the scheme: the angular [3,2-*h*] PPyQ **29** and the [1,4]diazepin-indole derivative **30**. All cyclization products were purified by re-crystallization from a suitable solvent or by flash chromatography, with their purity verified by HPLC (>95%).

2.2 Biological evaluation

2.2.1 In vitro antiproliferative activities and SAR analysis

The new compounds were designed to obtain additional SAR information by modifying the size of substituents at the 3 and 7 position of the aryl-PyQ tricycle, as well as the angular geometry. Evaluation of antiproliferative activities of **19-24, 26-27, 29** and **30** was performed with the 3-(4,5-dimethylthiazol-2-yl)-2,5-diphenyltetrazolium bromide (MTT) assay against a panel of 7 human tumor cell lines (HeLa, A549, HT-29, MDA-MB-231, RS4;11, Jurkat, and Kasumi-1). GI_{50} values, the concentrations that inhibit cell growth by 50%, are presented in Table 1. As reference

compound CA-4 was also added. From the cytotoxicity data reported in the Table, we can make some relevant remarks on SARs on the changed structural elements with respect to reference compound **31** (Figure 1). Regarding the 3-substituent on compounds **19** and **20**, replacing the ethyl group of **31** with a bulky linear alkyl chain (18 C) caused a massive loss of antiproliferative activity in all cell lines examined. This behavior was expected for **19**, which lacks the crucial phenyl in the 7 position, but this loss of activity was unexpected for **20**, which has the 7-phenyl group. In past studies [4], very high cytotoxicity was found for compounds with side chains up to 5 C at position 3 with a 7-phenyl. Compounds **21-24**, all bearing a 3-ethyl chain as in compound **31**, had nanomolar GI_{50}s, with compounds **21** and **24** all being especially active. These compounds all have even bulkier aryl 7-substituents than the 7-phenyl group, with the active **21** and **24** having, respectively, an α-naphthyland a benzodioxole substituent. In general, for angular [3,2-*f*] PPyQs such bulky groups are well tolerated. Of particular note, **21** and **24** had greater activity than **31,** in both the leukemic and solid tumor cell lines. In contrast, compound **22** with a 7-β-naphthyl substituent was 27-1430-fold less cytotoxic than compound **21**, depending on the cell line. In part, this must indicate a less favorable fit into the colchicine site relative to **21**. Cytotoxicity again increased with compound **23**, which had a 7-tetrahydronaphthyl substituent. Concerning the third structural element taken into consideration in this study, the configuration of the tricycle scaffold, the GI_{50}s obtained with compounds **26, 27** and **29** clearly indicate that the geometries [*f*] and [*g*] of **26** and **27**, respectively, produce at least one highly cytotoxic compound (nanomolar GI_{50}s), while the [*h*] geometry does not (compound **29)**. Compound **30**, a diazepine-indole derivative, was also tested, and it was completely inactive (GI_{50}s > 10000 nM).

*2.2.2 Evaluation of cytotoxicity of compounds **21** and **24** in human non-cancer cells*

To obtain a preliminary indication of the cytotoxic potential of these derivatives in normal human cells, two of the most active compounds (**21** and **24**) were evaluated *in vitro* against peripheral blood lymphocytes (PBL) from healthy donors (Table 2). Compound **21** was completely inactive in quiescent lymphocytes (GI_{50}>100 μM), while in the presence of the mitogenic stimulus phytohematoaglutinin (PHA), the GI_{50} was about 25.7 μM. Notably, this value was almost 10000-30000 times higher than that observed against the lymphoblastic cell lines Jurkat and CEM (Tables 1 and 3). These results indicate that **21** has a modest inhibitory effect in rapidly proliferating non-cancer cells but not in quiescent cells, as previously observed for other antimitotic derivatives developed by our group [8,9]. Analogous behavior was observed for compound **24**, which showed a GI_{50} of 45.3 μM in quiescent lymphocytes, while, in the presence of (PHA, the GI_{50} decreased to about 23.0 μM.

*2.2.3 Effect of compounds**21** and **24** on multidrug resistant cells*

To investigate whether these derivatives are substrates of drug efflux pumps, two of the most active compounds (**21** and **24**) were tested against $CEM^{Vbl\text{-}100}$ cells that are a multidrug-resistant line selected against vinblastine [4] and that overexpress P-glycoprotein (P-gp). This membrane protein acts as a drug efflux pump and exhibits resistance to a wide variety of structurally unrelated anticancer drugs and other compounds. As shown in Table 3, both compounds exhibited cytotoxic activity in the CEM^{Vbl100} cell line that was even higher than their activity against the parental line. Thus, these derivatives are not substrates for P-gp.

2.2.4 Inhibition of tubulin polymerization and colchicine binding

To evaluate the tubulin interaction properties of compounds **21, 23, 24** and of the mixture **26-27**, we investigated their effects on the inhibition of tubulin polymerization and on the binding of

[^{3}H]colchicine to tubulin (Table 4) [12,13]. For comparison, CA-4 was examined in contemporaneous experiments as a reference compound along with compound **31**. Among the test compounds, **21** and **24** strongly inhibited tubulin assembly with IC_{50} below 1 μM (0.99 and 0.84 μM, respectively) but slightly higher than that obtained for the reference compounds CA-4 (IC_{50}=0.64 μM) and **31** (IC_{50}=0.57 μM). Compound **23** also inhibited tubulin assembly with a low IC_{50} value of 1.1 μM, while the mixture **26-27** had less activity, with an IC_{50} of 6.2 μM. The PPyQ compounds all inhibited the binding of [^{3}H]colchicine to tubulin, with the best activity occurring with **21** and **24**, but none approached CA-4 in its potency as an inhibitor of colchicine binding. These results with tubulin correlate well with the growth inhibitory effects exhibited by compounds **21, 23** and **24**, indicating that their antiproliferative activity derives mostly from an interaction with tubulin. For the mixture **26-27**, the correlation between cytotoxicity and inhibitory effects on tubulin is perhaps not as good and could indicate there is an additional mechanism of action for this compound.

*2.2.5 Influence of test compounds **21, 23** and **24** on the cell cycle*

The effect of compounds **21, 23** and **24** on cell cycle progression was examined by flow cytometry in Hela cells (Figure 2). After a 24 h treatment, all compounds induced a G2/M arrest, although compound **21** showed a more modest accumulation in G2/M cells than occurred with the other compounds. In contrast, compounds **23** and **24** induced a greater G2/M block even at lower concentrations. A concomitant reduction of both the S and G1 phases was also observed.

We also studied the association between **24**-induced G2/M arrest and alterations in G2/M regulatory protein expression in HeLa cells. As shown in Figure 3, compound **24** caused, in a time- and concentration-dependent manner, an increase in cyclin B1 expression after 24 and 48 h, indicating an activation of the mitotic checkpoint following drug exposure. This effect was confirmed by a

reduction in the expression of phosphatase cdc25c at 24 h, followed by a disappearance in its expression at 48 h. This was associated with the appearance of slower migrating forms of phosphatase cdc25c indicative of cdc25c phosphorylation. The phosphorylation of cdc25c directly stimulates its phosphatase activity, and this is necessary to activate cdc2/cyclin B on entry into mitosis [14,15].We also observed a decrease of the phosphorylated form of cdc2 kinase, in particular after the 48 h treatment.

*2.2.6 Compounds **21**, **23** and **24** induce apoptosis in different cell lines*

To evaluate the mode of cell death induced by test compounds, we performed a bi-parametric cytofluorimetric analysis using propidium iodide (PI) and annexin-V-FITC, which stain DNA and phosphatidylserine (PS) residues, respectively. We used two cell lines, Hela and A549, in which we evaluated the effects of compounds **21**, **23** and **24**. In additional experiments we have also evaluated the apoptotic response of CA-4, as reference compounds, in HeLa cells. As shown in Figure 4, the three compounds had different potencies. In both cell lines, the compounds induced apoptosis in a time and concentration dependent manner, with compounds **21** and **24** being the most active compounds in good agreement with the cytotoxicity data. To note, that CA-4 induce a strong apoptotic response at the concentration of 0.1 μM in HeLa cells in well agreement with previous reports [16,17]

*2.2.7 Compound **24** induced mitochondrial depolarization and reactive oxygen species (ROS) production*

Mitochondria play an essential role in the propagation of apoptosis [18,19]. It is well established that, at an early stage, apoptotic stimuli alter the mitochondrial transmembrane potential ($\Delta\psi_{mt}$).

$\Delta\psi_{mt}$ was monitored by the fluorescence of the dye JC-1 [20]. HeLa cells treated with compound **24** (0.1-1.0 μM) showed a time-dependent increase in the percentage of cells with low $\Delta\psi_{mt}$ (Figure 4, Panel A). The depolarization of the mitochondrial membrane is associated with the appearance of annexin-V positivity in the treated cells when they are in an early apoptotic stage. In fact, the dissipation of $\Delta\psi_{mt}$ is characteristic of apoptosis and has been observed with both microtubule stabilizing and destabilizing agents, including other derivatives, in different cell types [21-24]. It is well known that mitochondrial membrane depolarization is associated with the mitochondrial production of ROS [25,26]. Therefore, we investigated whether ROS production increased after treatment with the test compounds. We utilized the fluorescence indicator 2,7-dichlorodihydrofluorescein diacetate (H_2-DCFDA) [27]. As shown in Figure 4 (Panel B) compound **24** induced significant production of ROS starting at 12-24 h of treatment at 1 μM, in good agreement with the mitochondrial depolarization described above.

*2.2.8 Compound **24** induced PARP activation and caused a decrease in the expression of anti-apoptotic proteins*

As shown in Figure 5, compound **24** in HeLa cells caused a concentration and time-dependent cleavage of poly (ADP-Ribose) polymerase (PARP), confirming its pro-apoptotic activity.

We also investigated the expression of anti-apoptotic proteins, such as Bcl-2 and Mcl-1. Bcl-2 play a major role in controlling apoptosis through the regulation of mitochondrial processes and the release of mitochondrial proapoptotic molecules that are important for the cell death pathway [28-30]. Our results (Figure 6) showed that the expression of the anti-apoptotic protein Bcl-2 was decreased starting after a 24 h treatment at both concentration used (0.1 and 1.0 μM). The decrease in expression of Mcl-1 was even greater.

2.3 Computational Studies

Molecular docking studies were carried out to investigate the possible binding mode of the novel inhibitors with the aim of interpreting the biological data. Recently, we reported a study that identified two fundamental aspects of the interaction of 7-PPyQ derivatives with tubulin that enhanced our ability to obtain reliable docking results: which protein conformation is most suitable to accommodate the 7-PPyQ scaffold and which docking protocol performs best in reproducing the experimental structure of the complexes associated with that protein conformation [9]. Taking advantage of these findings, we docked eight of our derivatives, **19-24** and **29-30**. As with the previously reported 7-PPyQ derivatives and, by analogy, with plinabulin [31], we observed that the most potent compounds **21**, **23**, and **24** occupied the colchicine site by establishing and maintaining a key hydrogen bond interaction with the backbone of βVal236 mediated by the pyrroloquinolinone scaffold. The fused-ring system, in addition, guaranteed strong hydrophobic interactions with βLeu253, βAla314, and βIle368. The substituents in position 7 established hydrophobic interactions with residues βPhe167, βTyr200, and βLeu250. The alkyl substituents at the *N*-pyrrole were placed in the pocket formed by residues βLys350, βThr351, βAla314, βAla352, and βThr179. Among the newly synthesized compounds, most of the small structural differences that caused strong divergences in activity are nicely explained by molecular docking (Video-S1). Compounds **21** and **22** only differ in the position of the conjugation of the naphthyl group in alpha and in beta position, respectively. While **21** preserves the typical interaction scheme, and, in particular, the hydrogen bond with βVal236, compound **22** fails to achieve a similar interaction (Figure 7). More subtle structural differences, as with compounds **22-24**, are more difficult to rationalize, even in terms of the shape of their substituent at position 7 (Figure 7). While the most active derivative **24** is able, through the benzodioxole group to establish a further hydrogen bond with βGln134 in addition to the typical hydrogen mediated by the pyrroloquinolinone core with βVal236 (Figure 7), both **22** and **23** fail to display the usual interaction with βVal236. The differences between the naphthyl and

tetrahydronaphthyl substituents are minimal, but these differences abolish the activity of **22**. However, it is difficult to ascribe the diverse biological effects to such small structural difference. Derivatives with a bulky substituent at the *N*-pyrrole apparently are able to retain the interaction pattern that occurs with the most potent compounds, **21**, **23**, and **24**. Docking results suggest that such derivatives could theoretically be accommodated in the colchicine site and reproduce the binding mode of the most potent derivatives. The long linear alkyl chain (18 carbon atoms) characterizing analogs **19** and **20** may protrude between the beta-strand 373-381 and the alpha helix 252-259 and interact with the α-tubulin subunit. However, such a hydrophobic group would drastically affect the physicochemical properties of these compounds. The logP reaches values of 7.15 and 7.69 for **19** and **20**, respectively (Table S1), suggesting a plausible sequestration by the membrane. Molecular docking also revealed that alternative scaffold geometries like the angular [3,2-*h*] PPyQ **29** and the [1,4]diazepin-indole derivative **30** were not able to reproduce the interaction pattern of the most potent compounds (per-residue interaction heat map profile, Video S1).

3. Conclusion

Continuing our research aimed to expand our understanding of the SAR data of PPyQs, we synthesized a small library of analogs by chemically modifying three structural elements: substituents on the 3N pyrrole (**19** and **20**), varying the aryl group at the 7 position (**21-24**) and the [3,2-f] angular geometry (**26-29**). Evaluation of antiproliferative activity by the MTT test indicated that extensive elongation of the alkyl chain bound to 3N sharply decreased cytotoxicity (**19** and **20**), while enlargement of the aryl moiety at position 7 could increase cytotoxicity (**21, 23** and **24**) . The un-separable mixture of compounds **26** and **27** showed that [*f*] and/or [*g*] angular geometries, respectively, could result in high cytotoxic activity, while compound **29**, with [*h*] angular geometry did not. Compounds **21, 23** and **24** were the most cytotoxic compounds (nanomolar GI_{50}s) among

the newly synthesized compounds, and they acted by an apoptotic mechanism and were excellent inhibitors of tubulin polymerization through an interaction at the colchicine site.

In addition, compounds **21** and **24** showed only modest effects in a rapidly proliferating noncancer cell and were completely inactive in quiescent cells. Both derivatives were not substrates for the Pgp drug efflux pump, as shown by their excellent cytotoxic activity against the multidrug-resistant CEM^{Vbl100} cell line. Compound **24** also induced mitochondrial depolarization and ROS production, PARP activation and decreased expression of anti-apoptotic proteins. The molecular docking studies of all derivatives showed that they could bind into the colchicine site in a manner similar to that of previously studied PPyQs [9]. Furthermore, the molecular docking studies provided good explanations for the effects of different substituents on the PPyQ nucleus. In particular, the molecular docking study revealed that the most active derivative **24** (sub-nanomolar GI_{50}s) is able through the benzodioxole group to establish an additional hydrogen bond with β-tubulin. Taking into account all of our results presented here, from a SAR point of view, compound **24** represents enhancement of the pharmacodynamics optimization process of the antimitotic PPyQ class, and it therefore merits *in vivo* evaluation.

4. Experimental Section

4.1 Chemistry

Melting points were determined on a Buchi M-560 capillary melting point apparatus and are uncorrected. Infrared spectra were recorded on a PerkinElmer 1760 FTIR spectrometer with potassium bromide pressed disks; all values are expressed in cm−1. UV−vis spectra were recorded on a Thermo Helyos α spectrometer. ^{1}H NMR spectra were determined on Bruker 300 and 400 MHz spectrometers, with the solvents indicated; chemical shifts are reported in δ (ppm) downfield from tetramethylsilane as internal reference. Coupling constants are given in hertz. In the case of multiplets, chemical shifts were measured starting from the approximate centre. Integrals were

satisfactorily in line with those expected based on compound structure. Mass spectra were obtained on a Mat 112 Varian Mat Bremen (70 eV) mass spectrometer and Applied Biosystems Mariner System 5220 LC/MS (nozzle potential 140 eV). Column flash chromatography was performed on Merck silica gel (250−400 mesh ASTM); chemical reactions were monitored by analytical thin-layer chromatography (TLC) on Merck silica gel 60 F-254 glass plates. Microwave assisted reactions were performed on a CEM Discover® monomode reactor with a built-in infrared sensor assisted-temperature monitoring and automatic power control; all reactions were performed in closed devices under pressure control. Solutions were concentrated on a rotary evaporator under reduced pressure. The purity of new tested compounds was checked by HPLC using the instrument HPLC VARIAN ProStar model 210, with detector DAD VARIAN ProStar 335. The analysis was performed with a flow of 1 mL/min, a C-18 column of dimensions 250 mm x 4.6 mm, a particle size of 5 mm, and a loop of 10 µL. The detector was set at 300 nm. The mobile phase consisted of phase A (Milli-Q H_2O, 18.0 MU, TFA 0.05%) and phase B (95% MeCN, 5% phase A). Gradient elution was performed as reported: 0 min, % B = 10; 20 min, % B = 90; 25 min, % B = 90; 26 min, % B = 10; 31 min, % B = 10.

Starting materials were purchased from Sigma-Aldrich and Alfa Aesar, and solvents were from Carlo Erba, Fluka and Lab-Scan. DMSO was obtained anhydrous by distillation under vacuum and stored over molecular sieves.

4.1.1 General Procedure for the Synthesis of 1N-Substituted Nitroindoles (**1**-**4**). As a typical procedure, the synthesis of 5-nitro-1-octadecyl-1*H*-indole **1** is described in detail. Into a two-necked 100 mL round-bottomed flask, 0.333 g (13.88 mmol) of NaH, 60% dispersion in mineral oil, was placed and washed with toluene (3 × 10 mL). With stirring, a solution of commercial 5-nitroindole, 0.750 g (4.625 mmol), in 5 mL of anhydrous DMF, was dropped into the flask, and the initial yellow color changed to red with the formation of H_2 gas. After 40 min at room temperature, the mixture was cooled to 0 °C, and 2.36 mL (6.94 mmol, d=0.849 g/mL) of 1-chlorooctadecane was

dropped into the flask and 0.050 g of NaI were added to the mixture. The reaction was monitored by TLC analysis (eluent toluene/*n*-hexane/ethyl acetate, 1:1:1). At the end of the reaction, 25 mL of water was added, and the solvent was evaporated under reduced pressure, leaving a residue that was extracted with ethyl acetate (3 × 50 mL). The organic phase, washed with water and brine and dried over anhydrous Na_2SO_4, was concentrated under vacuum giving a crude yellow solid (2.522 g). This crude product was purified with a silica gel chromatographic column (d 3 cm, l 35 cm, 230-400 mesh, eluent *n*-hexane/toluene, 1:1), yielding 1.618 g of a pure yellow powder.

4.1.1.1 5-nitro-1-octadecyl-1H-indole (**1**). Yield: 84.5 %; R*f*: 0.48 (*n*-hexane/toluene, 1:1); ^{1}H NMR (400 MHz, $CDCl_3$): δ 0.90 (t, J = 6.86 Hz, 3 H, N-$CH_2CH_2(CH_2)_{15}CH_3$), 1.26-1.33 (m, 30 H, N-$CH_2CH_2(CH_2)_{15}CH_3$), 1.87 (quin, J = 7.12 Hz, 2H, N-$CH_2CH_2(CH_2)_{15}CH_3$), 4.17 (t, J = 7.16 Hz, 2H, N-$CH_2CH_2(CH_2)_{15}CH_3$), 6.69 (dd, J= 3.22, 0.74 Hz, 1H, H-3), 7.26 (d, J = 3.24 Hz, 1H, H-2), 7.37 (d, J = 9.08 Hz, 1H, H-7), 8.13 (dd, J=9.10, 2.22 Hz, 1H, H-6), 8.61 (d, J = 2.24 Hz, 1H, H-4) ppm; ^{13}C NMR (101 MHz, $CDCl_3$): δ 14.11 (N-$CH_2CH_2(CH_2)_{15}CH_3$), 22.68 (N-$CH_2CH_2(CH_2)_{15}CH_3$), 26.89 (N-$CH_2CH_2(CH_2)_{15}CH_3$), 29.15 (N-$CH_2CH_2(CH_2)_{15}CH_3$), 29.35 (N-$CH_2CH_2(CH_2)_{15}CH_3$), 29.43 (N-$CH_2CH_2(CH_2)_{15}CH_3$), 29.50 (N-$CH_2CH_2(CH_2)_{15}CH_3$), 29.57 (N-$CH_2CH_2(CH_2)_{15}CH_3$), 29.62 (N-$CH_2CH_2(CH_2)_{15}CH_3$), 29.65 (N-$CH_2CH_2(CH_2)_{15}CH_3$), 29.68 (N-$CH_2CH_2(CH_2)_{15}CH_3$), 30.21 (N-$CH_2CH_2(CH_2)_{15}CH_3$), 31.92 (N-$CH_2CH_2(CH_2)_{15}CH_3$), 46.92 (N-$CH_2CH_2(CH_2)_{15}CH_3$), 103.85 (C-3), 109.18 (C-7), 117.13 (C-6), 118.27 (C-4), 127.69 (C-3a), 130.92 (C-2), 138.81 (C-7a), 141.50 (C-5) ppm.

4.1.1.2 1-ethyl-5-nitro-1H-indole (**2**). Compound **2** was prepared as for compound **1** by reacting commercial 5-nitroindole (1.50 g, 9.25 mmol), NaH (0.666 g, 27.75 mmol), and bromoethane (1.04 mL, 13.88 mmol) in DMF at room temperature. The reaction was monitored by TLC analysis (eluent toluene/*n*-hexane/ethyl acetate, 1:1:1). At the end of the reaction, the mixture was extracted to yield 1.649 g of yellow solid product. Yield: 93.7%; R*f*: 0.67 (toluene/*n*-hexane/ethyl acetate,

1:1:1); ^{1}H NMR (300 MHz, DMSO-d_6): δ 0.55 (t, J = 7.1 Hz, 3H, CH_3), 3.47 (q, J = 7.1 Hz, 2H, CH_2), 5.93 (d, J = 3.3 Hz, 1H, H-2), 6.87 (m, 2H, H-7 e H-3), 7.20 (dd, J = 9.0, 2.1 Hz, 1H, H-6), 7.74 (d, J = 2.1 Hz, 1H, H-4) ppm.

4.1.1.3 1-ethyl-6-nitro-1H-indole (**3**). Compound **3** was prepared as for compound **1** by reacting commercial 6-nitroindole (1.00 g, 6.17 mmol), NaH (0.444 g, 18.50 mmol), and bromoethane (0.69 mL, 9.25 mmol) in DMF at room temperature. The reaction was monitored by TLC analysis (eluent toluene/*n*-hexane/ethyl acetate, 1:1:1). At the end of the reaction, the mixture was extracted to yield 1.110 g of yellow solid. Yield: 94.5 %; R*f*: 0.75 (toluene/*n*-hexane/ethyl, 1:1:1); ^{1}H NMR (300 MHz, $CDCl_3$): δ 1.45 (t, J = 7.29 Hz, 3H, $CH_2C\mathit{H_3}$), 4.20 (q, J = 7.30 Hz, 2H, $C\mathit{H_2}CH_3$), 6.52 (dd, J = 3.07 Hz e J = 0.82 Hz, 1H, H-3), 7.34 (d, J = 3.09 Hz, 1H, H-2), 7.58 (d, J = 8.73 Hz, 1H, H-4), 7.93 (dd, J = 8.79 Hz e J = 2.04 Hz, 1H, H-5), 8.27 ppm (d, J = 1.95 Hz, 1H, H-7); ^{13}C NMR (75 MHz, $CDCl_3$): δ 15.60 ($CH_2\mathit{C}H_3$), 41.53 ($\mathit{C}H_2CH_3$), 102.28 (C-3), 106.40 (C-7), 114.85 (C-5), 120.80 (C-4), 132.83 (C-2), 133.41 (C-3a), 134.27 (C-7a), 142.85 (C-6) ppm.

4.1.1.4 1-ethyl-7-nitro-1H-indole (**4**). Compound **4** was prepared as for compound **1** by reacting commercial 7-nitroindole (1.00 g, 6.17 mmol), NaH (0.444 g, 18.50 mmol), and bromoethane (0.69 mL, 9.25 mmol) in DMF at room temperature. The reaction was monitored by TLC analysis (eluent toluene/*n*-hexane/ethyl acetate, 1:1:1). At the end of the reaction, the mixture was extracted to yield 1.103 g of yellow solid. Yield: 94.0 %; R*f*: 0.82 (toluene/*n*-hexane/ethyl acetate, 1:1:1); ^{1}H NMR (300 MHz, $CDCl_3$): δ 1.33 (t, J = 7.23 Hz, 3H, $CH_2C\mathit{H_3}$), 4.30 (q, J = 7.21 Hz, 2H, $C\mathit{H_2}CH_3$), 6.67 (d, J = 3.24 Hz, 1H, H-3), 7.14 (t, J = 7.84 Hz, 1H, H-5), 7.22 (d, J = 3.24 Hz, 1H, H-2), 7.82 (dd, J = 7.84, 0.82 Hz, 1H, H-4), 7.87 (dd, J = 7.78, 1.00 Hz, 1H, H-6) ppm; ^{13}C NMR (75 MHz $CDCl_3$): δ 16.01 ($CH_2\mathit{C}H_3$), 44.83 ($\mathit{C}H_2CH_3$), 103.01 (C-3), 118.40 (C-5), 119.78 (C-4), 126.13 (C-3a), 127.13 (C-6), 132.00 (C-2), 133.83 (C-7a), 136.87 (C-7) ppm.

4.1.2 *General Procedure for the Synthesis of 1N-Substituted Nitroindoles* (**5**-**8**). As a typical procedure, the synthesis of 1-octadecyl-1*H*-indol-5-amine **5** is described in detail. Into a two-necked flask, previously dried in an oven, about 0.300 g of Pd/C 10% and approximately 50 mL of ethyl acetate were placed. After connecting the flask to an elastomer balloon containing H_2, the mixture was stirred at room temperature for 1 h in order to saturate the suspension of Pd/C with H_2. Then, 1.00 g (2.41 mmol) of nitroindole derivative **1** in 15 mL of ethyl acetate was added dropwise to the suspension, and the mixture was stirred under H_2 at atmospheric pressure and heated by means of an oil bath at 50-60 °C, monitoring the progress of the reaction by TLC analysis (toluene/*n*-hexane, 1:1). At the end of the reaction, the mixture was filtered through a celite pad, and the solution was concentrated under vacuum to give 0.784 g of semisolid dark purple product.

4.1.2.1 1-octadecyl-1H-indol-5-amine (**5**). Yield: 84.8 %; R*f*: 0.12 (*n*-hexane:toluene, 1:1); ^{1}H NMR (400 MHz, $CDCl_3$)**:** δ 0.90 (t, J = 6.78 Hz, 3H, N-$CH_2CH_2(CH_2)_{15}CH_3$), 1.26-1.31 (m, 30H, N-$CH_2CH_2(CH_2)_{15}CH_3$), 1.82 (quin, J = 7.06 Hz, 2H, N-$CH_2CH_2(CH_2)_{15}CH_3$), 4.05 (t, J = 7.12 Hz, 2H, N-$CH_2CH_2(CH_2)_{15}CH_3$), 6.31 (d, J = 3.04 Hz, 1H, H-3), 6.72 (dd, J = 8.58, 2.22 Hz, 1H, H-6), 6.98 (d, J = 2.16 Hz, 1H, H-4), 7.03 (d, J = 3.04 Hz, 1H, H-2), 7.17 ppm (d, J = 8.60 Hz, 1H, H-7); ^{13}C NMR (101 MHz, CDCl3)**:** δ 14.11 (N-$CH_2CH_2(CH_2)_{15}CH_3$), 22.69 (N-$CH_2CH_2(CH_2)_{15}CH_3$), 27.01 (N-$CH_2CH_2(CH_2)_{15}CH_3$), 29.26 (N-$CH_2CH_2(CH_2)_{15}CH_3$), 29.36 (N-$CH_2CH_2(CH_2)_{15}CH_3$), 29.50 (N-$CH_2CH_2(CH_2)_{15}CH_3$), 29.57 (N-$CH_2CH_2(CH_2)_{15}CH_3$), 29.61 (N-$CH_2CH_2(CH_2)_{15}CH_3$), 29.64 (N-$CH_2CH_2(CH_2)_{15}CH_3$), 29.66 (N-$CH_2CH_2(CH_2)_{15}CH_3$), 29.67 (N-$CH_2CH_2(CH_2)_{15}CH_3$), 29.69 (N-$CH_2CH_2(CH_2)_{15}CH_3$), 30.26 (N-$CH_2CH_2(CH_2)_{15}CH_3$), 31.93 (N-$CH_2CH_2(CH_2)_{15}CH_3$), 46.50 (N-$CH_2CH_2(CH_2)_{15}CH_3$), 99.52 (C-3), 106.21 (C-4), 109.93 (C-7), 112.48 (C-6), 128.21 (C-2), 129.39 (C-3a), 131.29 (C-7a), 138.36 (C-5) ppm.

4.1.2.2 1-ethyl-1H-indol-5-amine (**6**). Compound **6** was prepared as for compound **5** by reacting 1.65 g of compound **2** (8.67 mmol), obtaining 1.36 g of a semisolid purple compound. Yield: 97.9

%; R*f*: 0.28 (toluene/*n*-hexane/ethyl, 1:1:1); ^{1}H NMR (300 MHz, DMSO-d_6): δ 1.55 (t, J = 7.3 Hz, 3H, CH_3), 4.06 (q, J = 7.3 Hz, 2H, CH_2), 4.48 (s br, 2H, NH_2), 6.15 (d, J = 3.05 Hz, 1H, H-2), 6.54 (dd, J = 8.5, 2.28 Hz, 1H, H-6), 6.69 (d, J = 2.28 Hz, 1H, H-4), 7.16 (m, 2H, H-3 e H-7) ppm.

4.1.2.3 1-ethyl-1H-indol-6-amine (**7**). Compound **7** was prepared as for compound **5** by reacting 1.45 g of compound **3** (7.61 mmol), obtaining 1.26 g of a semisolid purple compound. Yield: 99.8 %; R*f*: 0.28 (toluene/*n*-hexane/ethyl acetate, 1:1:1); ^{1}H NMR (300 MHz, $CDCl_3$): δ 1.33 (t, J = 7.26 Hz, 3H, CH_2CH_3), 3.42 (s, 2H, NH_2), 3.95 (q, J = 7.26 Hz, 2H, CH_2CH_3), 6.28 (d, J = 3.00 Hz, 1H, H-3), 6.47 (dd, J = 8.29, 2.95 Hz, 1H, H-5), 6.54 (d, J = 1.94 Hz, 1H, H-7), 6.83 (d, J = 3.29 Hz, 1H, H-2), 7.31 ppm (d, J = 8.31 Hz, 1H, H-4); ^{13}C NMR (75 MHz, $CDCl_3$): δ 15.30 (CH_2CH_3), 40.80 (CH_2CH_3), 94.95 (C-7), 100.94 (C-3), 110.29 (C-5), 121.57 (C-4), 122.03 (C-3a), 125.14 (C-2), 136.91 (C-7a), 141.69 (C-6) ppm.

4.1.2.4 1-ethyl-1H-indol-7-amine (**8**). Compound **8** was prepared as for compound **5** by reacting 1.43 g of compound **3** (7.64 mmol), obtaining 1.34 g of a semisolid purple compound. Yield: 99.8 %; R*f*: 0.48 (toluene/*n*-hexane/ethyl acetate, 1:1:1); ^{1}H NMR (300 MHz, $CDCl_3$): δ 1.51 (t, J = 7.23 Hz, 3H, CH_2CH_3), 3.72 (s, 2H, NH_2), 4.43 (q, J = 7.21 Hz, 2H, CH_2CH_3), 6.45 (d, J = 3.09 Hz, 1H, H-3), 6.53 (dd, J = 7.36, 0.88 Hz, 1H, H-4), 6.93 (dd, J = 7.83, 7.44 Hz, 1H, H-5), 7.01 (d, J = 3.12 Hz, 1H, H-2), 7.17 ppm (dd, J = 7.92, 1.05 Hz, 1H, H-6); ^{13}C NMR (75 MHz $CDCl_3$): δ 18.13 (CH_2CH_3), 43.87 (CH_2CH_3), 101.64 (C-3), 110.20 (C-4), 113.23 (C-6), 120.19 (C-5), 126.52 (C-3a), 128.74 (C-2), 131.19 (C-7a), 132.14 (C-7) ppm.

4.1.3 *General Procedure for the Synthesis of Aryl Ethyl Acetate Derivatives* **9**-**12**. As a typical procedure, the preparation of aryl ethyl acetate derivative **9** is described in detail. 2.36 g (98.33 mmol) of NaH 60% dispersion in mineral oil was placed in a 100 mL round-bottomed flask and washed with toluene to remove oil. Then, 7.12 mL (59.75 mmol, d=0.975 g/mL) of diethyl

carbonate and 20 mL of anhydrous dioxane were added. The mixture was heated to 80 °C with stirring and then 4.46 mL (29.37 mmol, d=1.120 g/mL) of 1-acetyl naphthalene was added dropwise. The mixture was stirred at 80 °C for 15 h and monitored by TLC analysis (eluent ethyl acetate/petroleum ether, 1:5). The reaction mixture was allowed to cool to room temperature, and 25 mL of water was added. The water layer was separated and extracted twice with ethyl acetate. The organic layers were combined and washed with water and brine, dried over Na_2SO_4, filtered, and evaporated to dryness, giving 5.73 g of a yellow oil. The crude product was used for the next reaction step without further purification.

4.1.3.1 Ethyl 3-(naphthalen-5-yl)-3-oxopropanoate (**9**). Yield: 80.52%; R*f*: 0.68 (EtOAc:petroleum ether, 1:5); ^{1}H-NMR (DMSO-d_6)= δ 1.11 (t, J = 7.09 Hz, 3H, $OCH_2C\mathit{H}_3$), 4.08 (q, J = 7.09 Hz, 2H, $OC\mathit{H}_2CH_3$), 4.30 (s, 2H, $COCH_2CO$), 7.68 (m, 3H, H-3, H-6, H-7), 8.03 (m, J = 8.84 Hz, 1H, H-8), 8.18 (m, J = 8.23 Hz, 2H, H-4, H-5), 8.57 (d, J = 8.39 Hz, 1H, H-2).

4.1.3.2 Ethyl 3-(naphthalen-6-yl)-3-oxopropanoate (**10**). Compound **10** was prepared as for compound **9** by reacting 2.5 g of commercial 2-acetyl-naphthalene (14.69 mmol) with 3.55 mL (29.31 mmol) of diethyl carbonate and 1.17 g (48.79 mmol) of NaH in 20 mL of dioxane to yield 2.45 g of crude product. This was purified by column chromatography (d 3 cm, l 35 cm, 230-400 mesh, eluent ethyl acetate/petroleum ether, 1:5), yielding 1.429 g of a yellow solid. Yield: 40.1 %; R*f*: 0.55 (EtOAc:petroleum ether, 1:5); ^{1}H NMR (300 MHz, $CDCl_3$): δ 1.19 (t, J = 7.14 Hz, 3H, $OCH_2C\mathit{H}_3$) 4.05 (s, 2H, $OC\mathit{H}_2O$), 4.16 (q, J = 7.13 Hz, 2H, OCH_2CH_3), 7.49-7.58 (m, 2H, H-6' e H-7'), 7.81 (d, J = 8.58 Hz, 1H, H-5'), 7.84 (d, J = 8.49 Hz, 1H, H-4'), 7.90 (d, J = 7.98 Hz, 1H, H-8'), 7.94 (dd, J=8.68, 1.78 Hz, 1H, H-3'), 8.38 (d, J = 1.26 Hz, 1H, H-1'). Keto-enol ratio 81:19.

4.1.3.3 Ethyl 3-(1,2,3,4-tetrahydronaphthalen-7-yl)-3-oxopropanoate (**11**). Compound **11** was prepared as for compound **9** by reacting 0.945 mL of commercial 6-acetyl-1,2,3,4-

tetrahydronaphthalene (5.74 mmol) with 1.39 mL (11.48 mmol) of diethyl carbonate and 0.457 g (19.06 mmol) of NaH in 20 mL of dioxane to yield 0.694 g of crude product. This was purified by column chromatography (d 3 cm, l 35 cm, 230-400 mesh, eluent ethyl acetate/petroleum ether, 1:5), yielding 0.351 g of a yellow solid. Yield: 24.8 %; R*f*: 0.78 (EtOAc:petroleum ether, 1:5); ^{1}H NMR (300 MHz, $CDCl_3$): δ 1.25 (t, J = 7.15 Hz, 3H, OCH_2CH_3), 1.81 (m, 4H, H-6' e H-7'), 2.81 (m, 4H, H-5' e H-8'), 3.94 (s, 2H, OCH_2O), 4.20 (q, J = 7.13 Hz, 2H, OCH_2CH_3), 7.14 (d, J = 8.61 Hz, 1H, H-4'), 7.63 (dd, J=7.18, 1.87 Hz, 1H, H-3'), 7.65 (m, 1H, H-1'). Keto-enol ratio 90:10.

4.1.3.4 Ethyl 3-(benzo[d][1,3]dioxol-6-yl)-3-oxopropanoate (**12**). Compound **12** was prepared as for compound **9** by reacting 1.642 g of commercial 1-(benzo[*d*][1,3]dioxol-6-yl)ethanone (10 mmol) with 2.42 mL (20 mmol) of diethyl carbonate and 0.672 g (28 mmol) of NaH in 20 mL of THF to yield 2.162 g of a yellow oil. The crude product is used for the next reaction step without further purification. Yield: 91.5 %; R*f*: 0.40 (EtOAc:petroleum ether, 1:5); ^{1}H NMR (300 MHz, $CDCl_3$): δ 1.25 (t, J = 7.14 Hz, 3H, OCH_2CH_3), 3.90 ($OCCH_2CO$), 4.19 (q, J = 7.14 Hz, 2H, OCH_2CH_3), 6.04 ($COCH_2OC$), 6.84 (d, J = 8.16 Hz, 1H, H-4'), 7.41 (d, J = 1.74 Hz, 1H, H-1'), 7.51 (dd, J = 8.17, 1.78 Hz, 1H, H-3'). Keto-enol ratio 95:5.

4.1.4 *General Procedure for the Synthesis of Acrylate Derivatives* **13-18, 25** and **28**. As a typical procedure, the synthesis of acrylate derivative **13** is described in detail. In a 100 mL round-bottomed flask, 0.786 g (2.045 mmol) of 3-substituted aminoindole **5** in 10 mL of absolute ethanol was condensed with 0.388 mL (3.07 mmol; d = 1.029 g/ mL) of commercial ethyl acetoacetate and 0.5 mL of glacial acetic acid in the presence of 100 mg of drierite. The mixture was refluxed for about 48 h, the reaction being monitored by TLC analysis (*n*-hexane/ethyl acetate, 8:2). At the end of the reaction, the mixture was cooled and filtered to remove the drierite. The resulting solution was evaporated to dryness under vacuum and the residue (1.039 g) purified by silica gel chromatography (d = 3 cm, l = 35 cm, 230−400 mesh, eluent *n*-hexane/ethyl acetate, 8:2) to yield

0.770 g of a semisolid brown product.

4.1.4.1 (E,Z)-ethyl 3-(1-octadecyl-1H-indol-5-ylamino)but-2-enoate (**13**). Yield: 75.8%; R*f*: 0.80 (*n*-hexane/ethyl acetate, 8:2); ^{1}H NMR (400 MHz, $CDCl_3$): δ 0.90 (t, J = 6.85 Hz, 3H, N-$CH_2CH_2(CH_2)_{15}CH_3$), 1.27-1.33 (m, 30H, N-$CH_2CH_2(CH_2)_{15}CH_3$), 1.31 (t, J = 7.10 Hz, 3H, $COOCH_2CH_3$), 1.85 (quin, J = 6.88 Hz, 2H, N-$CH_2CH_2(CH_2)_{15}CH_3$), 1.93 (s, 3H, $NHCCH_3$) 4.11 (t, J = 7.20 Hz, 2H, N-$CH_2CH_2(CH_2)_{15}CH_3$), 4.18 (q, J = 7.13 Hz, 2H, $COOCH_2CH_3$), 4.67 (s, 1H, NHCCH), 6.46 (d, J = 3.08 Hz,1H, H-3), 6.97 (dd, J=8.56, 1.96 Hz, 1H, H-6), 7.13 (d, J = 3.12 Hz, 1H, H-2), 7.28 (d, J = 8.56 Hz, 1H, H-7), 7.37 (d, J = 1.92 Hz, 1H, H-4) 10.28 ppm (s, 1H, NH); ^{13}C NMR (101 MHz, $CDCl_3$): δ 14.11 (N-$CH_2CH_2(CH_2)_{15}CH_3$), 14.67 ($COOCH_2CH_3$), 20.25 ($NHCCH_3$) 20.25 (N-$CH_2CH_2(CH_2)_{15}CH_3$), 22.68 (N-$CH_2CH_2(CH_2)_{15}CH_3$), 27.00 (N-$CH_2CH_2(CH_2)_{15}CH_3$), 29.23 (N-$CH_2CH_2(CH_2)_{15}CH_3$), 29.25 ($NCH_2CH_2(CH_2)_{15}CH_3$), 29.35 (N-$CH_2CH_2(CH_2)_{15}CH_3$), 29.49 (N-$CH_2CH_2(CH_2)_{15}CH_3$), 29.56 (N-$CH_2CH_2(CH_2)_{15}CH_3$), 29.61 (N-$CH_2CH_2(CH_2)_{15}CH_3$), 29.65 ($NCH_2CH_2(CH_2)_{15}CH_3$), 29.67 (N-$CH_2CH_2(CH_2)_{15}CH_3$), 29.69 (N-$CH_2CH_2(CH_2)_{15}CH_3$), 30.11 (N-$CH_2CH_2(CH_2)_{15}CH_3$), 30.26 (N-$CH_2CH_2(CH_2)_{15}CH_3$), 31.92 ($NCH_2CH_2(CH_2)_{15}CH_3$), 46.62 (N-$CH_2CH_2(CH_2)_{15}CH_3$), 58.50 ($COOCH_2CH_3$), 83.81 (NHCCH), 100.89 (C-3), 109.51 (C-7), 118.05 (C-4), 120.38 (C-6), 128.61 (C-3a), 128.83 (C-2), 131.16 (C-7a), 134.21 (C-5), 160.94 ($NHCCH_3$), 170.57 ($COOCH_2CH_3$) ppm.

4.1.4.2 (E,Z)-ethyl 3-(1-octadecyl-1H-indol-5-ylamino)-3-phenylacrylate (**14**). Compound **14** was prepared as for compound **13** by reacting 0.974 mL of commercial ethyl benzoylacetate (5.07 mmol, d = 1.11 g/mL) with 1.301 g (3.38 mmol) of previously prepared compound **5**, yielding 2.328 g of crude product, which was purified by silica gel column chromatography (d = 3 cm, l = 35 cm, 230−400 mesh, eluent *n*-hexane/ethyl acetate, 8:2) to yield 0.405 g of a semisolid brown product. Yield: 21.7%; R*f*: 0.77 (*n*-hexane/ethyl acetate, 8:2); ^{1}H NMR (300 MHz, $CDCl_3$): δ 0.80 (t, J = 6.70 Hz, 3H, N-$CH_2CH_2(CH_2)_{15}CH_3$), 1.18-1.16 (m, 30H, N-$CH_2CH_2(CH_2)_{15}CH_3$), 1.24 (t, J

= 7.10 Hz, 3H, $COOCH_2CH_3$) 1.68 (quin, J = 6.75 Hz, 2H, $N\text{-}CH_2CH_2(CH_2)_{15}CH_3$), 3.91 (t, J = 7.20 Hz, 2H, $NCH_2CH_2(CH_2)_{15}CH_3$), 4.13 (q, J = 7.11 Hz, 2H, $COOCH_2CH_3$), 4.85 (s, 1H, NHCCH), 6.19 (d, J = 3.03 Hz, 1H, H-3), 6.53 (dd, J=8.68, 2.11 Hz, 1H, H-6), 6.92 (d, J = 1.72 Hz, 1H, H-4), 6.93 (d, J = 3.12 Hz, 1H, H-2), 6.95 (d, J = 9.00 Hz, 1H, H-7), 7.13 (m, 1H, H-4'), 7.16 (m, 2H, H-3' e H-5'), 7.28 (m, 2H, H-2' e H-6'), 10.15 (s, 1H, NH) ppm. ^{13}C NMR (75 MHz, $CDCl_3$): δ 14.10 ($N\text{-}CH_2CH_2(CH_2)_{15}CH_3$), 14.67 ($COOCH_2CH_3$), 20.22 ($N\text{-}CH_2CH_2(CH_2)_{15}CH_3$), 22.98 ($N\text{-}CH_2CH_2(CH_2)_{15}CH_3$), 27.06 ($NCH_2CH_2(CH_2)_{15}CH_3$), 29.12 ($N\text{-}CH_2CH_2(CH_2)_{15}CH_3$), 29.34 ($N\text{-}CH_2CH_2(CH_2)_{15}CH_3$), 29.56 ($N\text{-}CH_2CH_2(CH_2)_{15}CH_3$), 29.67 ($NCH_2CH_2(CH_2)_{15}CH_3$), 29.76 ($N\text{-}CH_2CH_2(CH_2)_{15}CH_3$), 29.82 ($N\text{-}CH_2CH_2(CH_2)_{15}CH_3$), 29.84 ($N\text{-}CH_2CH_2(CH_2)_{15}CH_3$), 29.91 ($N\text{-}CH_2CH_2(CH_2)_{15}CH_3$), 30.23 ($NCH_2CH_2(CH_2)_{15}CH_3$), 30.67 ($N\text{-}CH_2CH_2(CH_2)_{15}CH_3$), 31.45 ($N\text{-}CH_2CH_2(CH_2)_{15}CH_3$), 46.16 ($N\text{-}CH_2CH_2(CH_2)_{15}CH_3$), 57.27 ($COOCH_2CH_3$), 84.18 (NHCCH), 104.28 (C-3), 113.28 (C-4), 114.27 (C-7), 116.28 (C-6), 124.82 (C-3a), 127.82 (C-2), 128.36 (C-2' e C-6'), 129.27 (C-3' e C-5') 130.17 (C-4'), 130.28 (C-7a), 131.01 (C-1'), 139.82 (C-5), 154.85 (NHCCH), 173.82 ($COOCH_2CH_3$) ppm.

4.1.4.3 (E,Z)-ethyl 3-(1-ethyl-1H-indol-5-ylamino)-3-(naphthalen-1-yl)acrylate (**15**). Compound **15** was prepared as for compound **13** by reacting 1.815 g (7.49 mmol) of compound **9** with 1 g (6.24 mmol) of previously prepared compound **6**, giving 2.461 g of crude product, which was purified by silica gel column chromatography (d = 3 cm, l = 35 cm, 230−400 mesh, eluent *n*-hexane/ethyl acetate/toluene, 1:1:1) to yield 0.879 g of a semisolid brown product. Yield: 36.6%; R*f*: 0.82 (*n*- / acetate, 8:2); ^{1}H NMR (400 MHz, DMSO-d_6): δ 1.21 (t, J = 7.16 Hz, 3H, $COOCH_2CH_3$), 1.41 (t, J = 7.20 Hz, 3H, NCH_2CH_3), 4.19 (q, J = 7.14 Hz, 2H, $COOCH_2CH_3$), 4.35 (q, J = 7.22 Hz, 2H, NCH_2CH_3), 4.92 (s, 1H, NHCCH), 7.24 (d, J = 2.12 Hz, 1H, H-5), 7.43 (dd, J = 8.81 Hz, 1H, H-6), 7.59 (m, 1H, H-3), 7.85 (m, 1H, H-2), 7.90 (dd, J = 8.95, 0.64 Hz, 1H, H-7), 8.08 (m, J = 8.56 Hz e J=2.14 Hz, 1H, H-8'), 8.13 (m, J=8.23 Hz, 1H, H-2'), 11.93 ppm (s, 1H, NH); ^{13}C NMR (101 MHz, DMSO-d6): δ 16.39 ($NHCH_2CH_3$), 17.04 ($COOCH_2CH_3$), 41.03 (NCH_2CH_3), 60.04

(COO*C*H_2CH_3), 88.94 (NHC*C*H), 104.10 (C-3), 112.53 (C-6), 115.98 (C-7), 118.31 (C-4), 123.64 (C-3a), 125.30 (C-2), 125.87 (C-aro), 126.94 (Caro), 127.64 (C-aro), 127.77 (C-aro), 128.64 (C-aro), 128.92 (C-8'), 130.12 (C-2'), 131.06 (C-8'a), 131.46 (C-4'), 132.44 (C-7a), 133.61 (C-1'), 147.37 (C-5), 153.12 (NH*C*CH), 170.24 (CO).

4.1.4.4 (E,Z)-ethyl 3-(1-ethyl-1H-indol-5-ylamino)-3-(naphthalen-3-yl)acrylate (**16**). **16** was prepared as for compound **13** by reacting 1 g (4.13mmol) of compound **10** with 0.440 g (2.75 mmol) of previously prepared compound **6**, giving 1.567 g of crude product, which was purified by silica gel column chromatography (d = 3 cm, l = 35 cm, 230−400 mesh, eluent *n*- /ethyl acetate 8:2) to yield 0.692 g of a semisolid orange product. Yield: 65.5%; R*f*: 0.44 (*n*-hexane/ethyl acetate, 8:2); ^{1}H NMR (300 MHz, $CDCl_3$): δ 1.19 (t, J = 7.12 Hz, 3H, NCH$_2$C*H*$_3$), 1.30 (t, J = 7.26 Hz, 3H, COOCH$_2$C*H*$_3$), 3.95 (q, J = 7.27 Hz, 2H, NC*H*$_2$CH$_3$), 4.16 (q, J =7.12 Hz, 2H, COOC*H*$_2$CH$_3$), 4.98 (s, 1H, NHCC*H*), 6.17 (dd, J = 3.09, 0.51 Hz, 1H, H-3), 6.58 (dd, J = 8.73, 2.07 Hz, 1H, H-6), 7.00 (dd, J=1.47 Hz, 1H, H-4), 7.24 (dd, J = 8.53, 1.69 Hz, 1H, H-3'), 7.38 (m, 1H, H-7'), 7.39 (d, J = 2.97 Hz, 1H, H-2), 7.46 (m, 1H, H-6), 7.84 (d, J = 8.49 Hz, 1H, H-7), 7.92 (m, 1H, H-5'), 7.93 (m, 1H, H-8'), 8.38 (s, 1H, H-1'), 10.39 (s, 1H, NH) ppm. ^{13}C NMR (75 MHz, $CDCl_3$): δ 15.92 (NCH$_2$*C*H$_3$), 16.38 (COOCH$_2$*C*H$_3$), 41.38 (N*C*H$_2$CH$_3$), 59.27 (COO*C*H$_2$CH$_3$), 90.28 (NHC*C*H), 101.27 (C-3), 109.27 (C-4), 115.88 (C-7), 116.27 (C-6), 126.93 (C-5'), 126.95 (C-6'), 127.27 (C-3'), 127.37 (C-2), 127.82 (C-7'), 127.82 (C-8'), 129.73 (C-4'), 129.81 (C-3a), 132.81 (C-7a), 133.82 (C-8'a), 133.98 (C-1'), 134.82 (C-4'a), 135.62 (C-2'), 142.73 (C-5), 149.12 (NH*C*CH), 175.98 (CO) ppm.

4.1.4.5 (E,Z)-ethyl 3-(1-ethyl-1H-indol-5-ylamino)-3-(1,2,3,4-tetrahydronaphthalen-7-yl)acrylate (**17**). Compound **17** was prepared as for compound **13** by reacting 0.373 g (1.51 mmol) of compound **11** with 0.201 g (1.26 mmol) of previously prepared compound **6**, giving 0.535 g of crude product, which was purified by silica gel column chromatography (d = 3 cm, l = 35 cm,

230−400 mesh, eluent *n*-hexane/ethyl acetate 8:2) to yield 0.337 g of a semisolid brown-orange product. Yield: 68.8%; R*f*: 0.54 (*n*-hexane/ethyl acetate, 8:2); ^{1}H NMR (300 MHz, $CDCl_3$): δ 1.19 (t, J = 7.14 Hz, 3H, NCH_2CH_3), 1.34 (t, J = 7.27 Hz, 3H, $COOCH_2CH_3$), 1.67 (m, 4H, H-6' e H-7'), 2.60 (m, 4H, H-5' e H-8'), 4.00 (q, J = 7.28 Hz, 2H, NCH_2CH_3), 4.13 (q, J = 7.11 Hz, 2H, $COOCH_2CH_3$), 4.83 (s, 1H, NHCCH), 6.23 (dd, J=3.07, 0.58 Hz, 1H, H-3), 6.57 (dd, J = 8.67, 2.10 Hz, 1H, H-6), 6.76 (d, J = 7.95 Hz, 1H, H-7), 6.97 (d, J = 2.91 Hz, 1H, H-1'), 7.07 (d, J = 8.55 Hz, 1H, H-3'), 7.42 (d, J = 1.56 Hz, 1H, H-4'), 7.57 (m, 1H, H-4'), 7.57 (m, 1H, H-2), 10.27 (s, 1H, NH) ppm; ^{13}C NMR (75 MHz, $CDCl_3$): δ 15.92 (NCH_2CH_3), 15.93 ($COOCH_2CH_3$), 24.96 (C-6' e C-7'), 30.04 (C-5' e C-8'), 40.72 (NCH_2CH_3), 61.38 ($COOCH_2CH_3$), 89.97 (NHCCH), 102.83 (C-3), 108.38 (C-4), 116.23 (C-6), 117.28 (C-7), 124.28 (C-3a), 124.82 (C-3'), 126.28 (C-1'), 127.28 (C-4'), 127.73 (C-2), 132.73 (C-7a), 135.28 (C-4'a), 136.93 (C-8'a), 139.83 (C-1'), 142.82 (C-5), 156.38 (NHCCH), 175.81 (CO) ppm.

4.1.4.6 (E,Z)-ethyl 3-(1-ethyl-1H-indol-5-ylamino)-3-(benzo[d][1,3]dioxol-6-yl)acrylate (**18**). Compound **18** was prepared as for compound **13** by reacting 1.130 g (4.79 mmol) of compound **12** with 0.639 g (3.99 mmol) of previously prepared compound **6**, giving 1.761 g of crude product, which was purified by silica gel column chromatography (d = 3 cm, l = 35 cm, 230−400 mesh, eluent *n*-hexane/ethyl acetate 8:2) to yield 0.558 g of a semisolid brown product. Yield: 16.1%; R*f*: 0.67 (*n*-hexane/ethyl acetate, 8:2); ^{1}H NMR (300 MHz, $CDCl_3$): δ 1.26 (t, J = 7.18 Hz, 3H, NCH_2CH_3), 1.37 (t, J = 7.23 Hz, 3H, $COOCH_2CH_3$), 4.08 (q, J = 7.28 Hz, 2H, NCH_2CH_3), 4.33 (q, J = 7.13 Hz, 2H, $COOCH_2CH_3$), 4.89 (s, 1H, NHCCH), 6.05 (s, 2H, OCH_2O), 6.31 (d, J=3.09 Hz, 1H, H-3), 6.65 (d, J = 8.10 Hz, 1H, H-7), 6.86 (d, J = 8.19 Hz, 1H, H-4'), 6.89 (dd, J = 8.09, 1.71 Hz, 1H, H-6), 7.02 (d, J = 2.01 Hz, 1H, H-4), 7.05 (d, J = 3.15 Hz, 1H, H-2), 7.43 (d, J = 1.69 Hz, 1H, H-1'), 7.53 (dd, J=8.17, 1.78 Hz, 1H, H-3'), 10.28 (s, 1H, NH) ppm; ^{13}C NMR (75 MHz, $CDCl_3$): δ 15.93 (NCH_2CH_3), 16.38 ($COOCH_2CH_3$), 41.28 (NCH_2CH_3), 61.28 ($COOCH_2CH_3$), 90.03 (NHCCH), 100.24 (OCH_2O), 104.28 (C-3), 108.28 (C-4), 110.28 (C-4'), 115.38 (C-7), 116.28

(C-6), 122.36 (C-3), 122.38 (C-3a), 124.73 (C-1), 127.82 (C-2), 135.47 (C-1'), 136.38 (C-7a), 142.38 (C-5), 147.28 (C-4'b), 148.37 (C-4a'), 157.38 (NH*C*CH), 174.28 (CO) ppm.

4.1.4.7 (E,Z)-ethyl 3-(1-ethyl-1H-indol-6-ylamino)-3-phenylacrylate (**25**). Compound **25** was prepared as for compound **13** by reacting 2.27 g of commercial ethyl benzoylacetate (11.79 mmol, d = 1.11 g/mL) with 1.26 g (7.86 mmol) of previously prepared compound **7**, giving 2.943 g of crude product, which was purified by silica gel column chromatography (d = 3 cm, l = 35 cm, 230−400 mesh, eluent *n*-hexane/ethyl acetate 6:4) to yield 2.069 g of a brown product. Yield: 78.7%; R*f*: 0.87 (*n*-hexane/ethyl acetate, 6:4); ^{1}H NMR (300 MHz, $CDCl_3$): δ 1.10 (t, J = 7.26 Hz, 3H, NCH_2CH_3), 1.25 (t, J = 7.12 Hz, 3H, $COOCH_2CH_3$), 3.78 (q, J = 7.27 Hz, 2H, NCH_2CH_3), 4.14 (q, J = 7.11 Hz, 2H, $COOCH_2CH_3$), 4.89 (s, 1H, NHCC*H*) 6.26 (dd, J=3.12, 0.75 Hz, 1H, H-3), 6.45 (d, J = 1.30 Hz, 1H, H-7), 6.51 (dd, J = 8.40, 1.92 Hz, 1H, H-5), 6.88 (d, J = 3.12 Hz, 1H, H-2), 7.16 (m, 1H, H-4'), 7.19 (m, 2H, H-3' e H-5'), 7.26 (d, J = 8.37 Hz, 1H, H-4), 7.30 (m, J = 8.77 Hz, 2H, H-2' e H-6'), 10.39 (s, 1H, NH) ppm; ^{13}C NMR (75 MHz, $CDCl_3$): δ 14.61 (NCH_2CH_3), 15.10 ($COOCH_2CH_3$), 40.91 (NCH_2CH_3), 59.19 ($COOCH_2CH_3$), 89.51 (NHC*C*H), 100.74 (C-3), 103.76 (C-7), 115.86 (C-5), 120.77 (C-4), 124.87 (C-3a), 127.10 (C-2), 128.29 (C-2' e C-6'), 128.39 (C-3' e C-5'), 129.11 (C-4'), 134.72 (C-1'), 135.51 (C-7a), 136.45 (C-6), 159.84 (NH*C*CH), 170.34 (CO) ppm.

4.1.4.8 (E,Z)-ethyl 3-(1-ethyl-1H-indol-7-ylamino)-3-phenylacrylate (**28**). Compound **28** was prepared as for compound **13** by reacting 2.418 g of commercial ethyl benzoylacetate (12.59 mmol, d = 1.11 g/mL) with 1.35 g (8.39 mmol) of previously prepared compound **8**, giving 3.166 g of crude product, which was purified by silica gel column chromatography (d = 3 cm, l = 35 cm, 230−400 mesh, eluent *n*-hexane/ethyl acetate 6:4) to yield 1.242 g of a brown product. Yield: 44.3%; R*f*: 0.84 (*n*-hexane/ethyl acetate, 6:4); ^{1}H NMR (300 MHz, $CDCl_3$): δ 1.28 (t, J = 7.14 Hz, 3H, NCH_2CH_3), 1.50 (q, J = 7.15 Hz, 2H, $COOCH_2CH_3$), 4.24 (q, J = 7.15 Hz, 2H, $COOCH_2CH_3$), 4.42 (q, J = 7.23 Hz, 2H, NCH_2CH_3), 5.13 (s, 1H, NHCC*H*), 6.44 (d, J = 3.12 Hz, 1H, H-3), 6.52

(dd, J = 7.35, 0.72 Hz, 1H, H-4), 6.91 (t, J = 7.63 Hz, 1H, H-5), 7.00 (d, J = 3.12 Hz, 1H, H-2), 7.16 (dd, J = 7.92, 0.87 Hz, 1H, H-6), 7.51 (m, J = 7.80 Hz, 2H, H-3' e H-5'), 7.62 (m, J=7.46, 2.05 Hz, 1H, H-4'), 7.97 (m, J =8.55 Hz, 2H, H-2' e H-6'), 10.62 ppm (s, 1H, NH); ^{13}C NMR (75 MHz, $CDCl_3$): δ 14.09 ($NCH_2\mathit{C}H_3$), 18.11 ($COOCH_2\mathit{C}H_3$), 43.86 (NCH_2CH_3), 61.52 ($COOCH_2CH_3$), 90.31 (NHC*C*H), 101.63 (C-3), 110.19 (C-4), 120.18 (C-5) 126.06 (C-3a), 128.52 (C-6) 128.56 (C-2), 128.72 (C-4'), 128.72 (C-6), 128.80 (C-3' e C-5'), 133.78 (C-1'), 135.94 (C-7a), 135.99 (C-7), 161.15 (NH*C*CH), 173.23 (CO) ppm.

4.1.5 *General Procedure for the Synthesis of Phenylpyrroloquinolinones* **19**-**24**, **26**, **27** *and* **29**. As a typical procedure, the synthesis of the phenylpyrroloquinolinone derivative **19** is described in detail. In a two-necked round-bottomed flask, 30 mL of diphenyl ether was heated to boiling. Acrylate derivative **13 (**0.758 g, 1.53 mmol) was then added portionwise, and the resulting mixture was refluxed for 15 min. After cooling to room temperature, 25 mL of diethyl ether was added, and the mixture was left for 12 h. The separated precipitate was collected by filtration and washed many times with diethyl ether. The crude product (0.534 g) was purified by flash column chromatography (eluent $CHCl_3$/methanol, 9:1), obtaining 0.165 g of a white powder.

4.1.5.1 7-methyl-3-octadecyl-3H-pyrrolo[3,2-f]quinolin-9(6H)-one (**19**). Yield: 23.6%; R*f*: 0.59 (blue fluorescent spot, $CHCl_3$/methanol, 9:1); mp = 140°C; ^{1}H NMR (400 MHz, $CDCl_3$): δ 0.89 (t, J = 6.84 Hz, 3H, N-$CH_2CH_2(CH_2)_{15}C\mathit{H_3}$), 1.31 - 1.25 (m, 30H, N-$CH_2CH_2(C\mathit{H_2})_{15}CH_3$), 1.86 (quin, J = 6.64 Hz, 2H, $NCH_2C\mathit{H_2}(CH_2)_{15}CH_3$), 2.45 (s, 3H, NHCC$\mathit{H_3}$), 4.21 (t, J = 7.06 Hz, 2H, $NC\mathit{H_2}CH_2(CH_2)_{15}CH_3$), 6.39 (s, 1H, H-8), 7.28 (d, J = 2.90 Hz, 1H, H-2), 7.63 (d, J = 9.00 Hz, 1H, H-4), 7.69 (d, J = 8.92 Hz, 1H, H-5), 7.83 (d, J = 2.88 Hz, 1H, H-1), 12.22 (s, 1H, NH) ppm; ^{13}C NMR (101 MHz, $CDCl_3$): δ 14.00 (N-$CH_2CH_2(CH_2)_{15}\mathit{C}H_3$), 19.67 (NHC$\mathit{C}H_3$), 22.48 (N-$CH_2CH_2(\mathit{C}H_2)_{15}CH_3$), 24.99 (N-$CH_2CH_2(\mathit{C}H_2)_{15}CH_3$), 26.74 ($NCH_2CH_2(\mathit{C}H_2)_{15}CH_3$), 29.03 (N-$CH_2CH_2(\mathit{C}H_2)_{15}CH_3$), 29.14 (N-$CH_2CH_2(\mathit{C}H_2)_{15}CH_3$), 29.29 (N-$CH_2CH_2(\mathit{C}H_2)_{15}CH_3$), 29.35 (N-

$CH_2CH_2(CH_2)_{15}CH_3$), 29.40 ($NCH_2CH_2(CH_2)_{15}CH_3$), 29.44 ($N\text{-}CH_2CH_2(CH_2)_{15}CH_3$), 29.48 ($N\text{-}CH_2CH_2(CH_2)_{15}CH_3$), 30.56 ($N\text{-}CH_2CH_2(CH_2)_{15}CH_3$), 31.71 ($N\text{-}CH_2CH_2(CH_2)_{15}CH_3$), 46.53 ($NCH_2CH_2(CH_2)_{15}CH_3$), 104.29 (C-1), 108.73 (C-8), 111.88 (C-5), 115.48 (C-4), 116.69 (C-9a), 122.92 (C-9b), 128.32 (C-2), 131.55 (C-3a), 136.44 (C-5a), 147.80 (C-7), 182.01 (C-9) ppm; IR (KBr): ν= 3391.59 (NH), 2919.43 (aliphatic C-H), 2847.80 (aliphatic C-H), 1637.16 (C=O), 1522.64 (C=C) cm^{-1}; UV-Vis (H_2O): 231.18 nm (A = 203.78 mAU), 275.70 nm (A = 93.22 mAU), 351.08 nm (45.03 mAU); fluorescence (MeOH): λ_{exc} = 350 nm, λ_{ems} = 416 nm; HRMS (ESI-MS, 140 eV): *m/z* $[M+H]^+$ calculated for $C_{30}H_{47}N_2O^+$, 451.3688; found, 451.3769; RP-C18 HPLC: t_R = 26.96 min, 99.9%.

4.1.5.2 3-octadecyl-7-phenyl-3H-pyrrolo[3,2-f]quinolin-9(6H)-one (**20**). Compound **20** was prepared as described for compound **19** by reacting 0.406 g (7.3 mmol) of the appropriate phenylacrylate derivative **14** to yield 0.389 g of a raw solid, which was purified by flash column chromatography (eluent $CHCl_3$/methanol, 95:5) to yield 0.175 g of a grey powder. Yield: 47.1%; R*f*: 0.38 (blue fluorescent spot, $CHCl_3$/methanol, 95:5); mp = 156°C; ^{1}H NMR (300 MHz, $CDCl_3$): δ 0.89 (t, J = 6.72 Hz, 3H, $N\text{-}CH_2CH_2(CH_2)_{15}CH_3$), 1.25-1.32 (m, 30H, $N\text{-}CH_2CH_2(CH_2)_{15}CH_3$), 1.88 (quin, J = 6.67 Hz, 2H, $NCH_2CH_2(CH_2)_{15}CH_3$), 4.24 (t, J = 7.15 Hz, 2H, $N\text{-}CH_2CH_2(CH_2)_{15}CH_3$), 6.65 (s br, 1H, H-8), 7.31 (m, 3H, H-3', H-4' e H-5'), 7.33 (d, J = 3.00 Hz, 1H, H-2), 7.65 (d, J = 7.29 Hz, 1H, H-4), 7.67 (m, 2H, H-2' e H-6'), 7.68 (d, J = 9.00 Hz, 1H, H-5), 7.84 (d, J = 2.91 Hz, 1H, H-1), ppm. ^{13}C NMR (75 MHz, $CDCl_3$): δ 14.02 ($N\text{-}CH_2CH_2(CH_2)_{15}CH_3$), 22.51 ($NCH_2CH_2(CH_2)_{15}CH_3$), 26.77 ($N\text{-}CH_2CH_2(CH_2)_{15}CH_3$), 29.07 ($N\text{-}CH_2CH_2(CH_2)_{15}CH_3$), 29.17 ($N\text{-}CH_2CH_2(CH_2)_{15}CH_3$), 29.18 ($N\text{-}CH_2CH_2(CH_2)_{15}CH_3$), 29.33 ($NCH_2CH_2(CH_2)_{15}CH_3$), 29.34 ($N\text{-}CH_2CH_2(CH_2)_{15}CH_3$), 29.38 ($N\text{-}CH_2CH_2(CH_2)_{15}CH_3$), 29.43 ($N\text{-}CH_2CH_2(CH_2)_{15}CH_3$), 29.46 ($N\text{-}CH_2CH_2(CH_2)_{15}CH_3$), 29.50 ($N\text{-}CH_2CH_2(CH_2)_{15}CH_3$), 30.60 ($NCH_2CH_2(CH_2)_{15}CH_3$), 31.73 ($N\text{-}CH_2CH_2(CH_2)_{15}CH_3$), 46.56 ($N\text{-}CH_2CH_2(CH_2)_{15}CH_3$), 104.42 (C-1), 108.28 (C-8), 112.66 (C-4), 115.48 (C-5), 117.75 (C-9a), 123.16 (C-9b), 127.10 (C-2'), 127.60 (C-6'), 128.31 (C-3'), 128.74 (C-

5'), 129.92 (C-2), 131.66 (C-4'), 134.75 (C-1'), 136.97 (C-3a), 139.18 (C-5a), 148.33 (C-7), 176.28 (C-9) ppm; IR (KBr): ν= 3403.42 (NH), 3090 (aliphatic C-H), 2903.12 (aliphatic C-H), 1651.15 (C=O), 1513.68 (C=C) cm^{-1}; UV-Vis (H_2O): 225.3 nm (A = 200.81 mAU), 276.10 nm (A = 197.23 mAU), 353.05 nm (76.28 mAU); fluorescence (MeOH): λ_{exc} = 350 nm, λ_{ems} = 458 nm; HRMS (ESI-MS, 140 eV): *m/z* $[M+H]^+$ calculated for $C_{35}H_{49}N_2O^+$, 513.3845; found, 513.3945; RP-C18 HPLC: t_R = 31.711 min, 98.02%.

4.1.5.3 3-ethyl-7-(naphthalen-1-yl)-3H-pyrrolo[3,2-f]quinolin-9(6H)-one (**21**). Compound **21** was prepared as described for compound **19** by reacting 0.877 g (2.28 mmol) of the appropriate phenylacrylate derivative **15** to yield 0.150 g of a yellow powder. Yield: 19.4 %; R*f*: 0.66 (light blue fluorescent spot, $CHCl_3$/methanol, 9:1); mp = 219°C; ^{1}H NMR (400 MHz, DMSO-d_6): δ 1.41 (t, J = 7.20 Hz, 3H, NCH_2CH_3), 4.34 (q, J = 7.22 Hz, 2H, NCH_2CH_3), 6.20 (s br, 1H, H-8), 7.43 (dd, J = 8.81 Hz, 1H, H-5), 7.52-7.75 (m, 5H, H-3', H-4', H-5', H-6' and H-7'), 7.59 (m, 1H, H-1) 7.85 (m, 1H, H-2), 7.90 (dd, J = 8.95, 0.64 Hz, 1H, H-4), 8.08 (m, J = 8.56, 2.14 Hz, 1H, H-8'), 8.13 (m, J = 8.23 Hz, 1H, H-2'), 12.01 (s br, 1H, NH) ppm; ^{13}C NMR (101 MHz, DMSO-d_6): δ 16.39 (NCH_2H_3), 41.03 (NCH_2CH_3), 104.10 (C-1), 111.58 (C-8), 112.53 (C-5), 115.98 (C-4), 118.31 (C-9a), 123.64 (C-9b), 125.30 (C-2), 125.87 (aromatic-C), 126.94 (aromatic-C), 127.64 (aromatic-C), 127.77 (aromatic-C), 128.64 (aromatic-C), 128.92 (C-8'), 130.12 (C-2'), 131.06 (C-8'a), 131.46 (C-4'a), 132.44 (C-3a), 133.61 (C-1'), 133.81 (C-7), 147.37 (C-5a), 178.15 (CO) ppm; IR (KBr): ν = 3436.75 (NH), 3024 (aliphatic C-H), 2974.66 (aliphatic C-H), 1608.39 (C=O), 1511.10 (C=C) cm^{-1}; UV-Vis (H_2O): 292 nm (A = 899 mAU), 340 nm (A = 501 mAU); fluorescence (MeOH): λ_{exc} = 350 nm, λ_{ems} = 479 nm; HRMS (ESI-MS, 140 eV): *m/z* $[M+H]^+$ calculated for $C_{23}H_{19}N_2O^+$, 339.1492; found, 339.1540; RP-C18 HPLC: t_R = 14.34 min, 95.13%.

4.1.5.4 3-ethyl-7-(naphthalen-3-yl)-3H-pyrrolo[3,2-f]quinoline-9(6H)-one (**22**). Compound **22** was prepared as described for compound **19** by reacting 0.297 g (0.77 mmol) of the appropriate

phenylacrylate derivative **16** to yield 0.270 g of a crude product, which was purified by flash column chromatography (eluent $CHCl_3$/methanol, 95:5) to yield 0.081 g of a dark yellow powder. Yield: 31%; R*f*: 0.43 (blue fluorescent spot, $CHCl_3$/methanol, 95:5); mp = 230°C; ^{1}H NMR (400 MHz, $CDCl_3$) δ 1.46 (t, *J* = 7.3 Hz, 3H, NCH_2CH_3), 4.19 (q, *J* = 7.3 Hz, 2H, NCH_2CH_3), 6.61 (s, 1H, H-8), 7.17 (m, 2H, H-1 and H-3'), 7.23 (d, *J* = 2.9 Hz, 1H, H-2), 7.44 (m, 5H, H-4, H-4', H-5, H-5'and H-6'), 7.83 (d, *J* = 2.8 Hz, 1H, H-7'), 8.00 – 7.93 (m, 2H, H-8' and H-1'), 11.24 (s, 1H, NH) ppm; ^{13}C NMR (75 MHz, $CDCl_3$): δ 15.90 (NCH_2CH_3), 41.21 (NCH_2CH_3), 104.82 (C-1), 108.46 (C-8), 113.13 (C-5), 115.46 (C-9a), 117.97 (C-4), 123.23 (C-9b), 124.18 (C-5'), 126.29 (C-6'), 126.72 (C-2), 127.15 (C-3'), 127.22 (C-4'), 127.39 (C-7'), 128.40 (C-8'), 128.44 (C-1'), 131.27 (C-8'a), 131.61 (C-4'a), 132.68 (C-2'), 133.40 (C-3a), 137.16 (C-5a), 148.56 (C-7), 178.27 (CO) ppm; IR (KBr): ν= 3432.76 (NH), 3034 (aliphatic C-H), 2955.07 (aliphatic C-H), 1605.36 (C=O), 1518.17 (C=C) cm^{-1}; UV-Vis (H_2O): 212 nm (A = 1.03 AU), 235.09 nm (A= 982.95 mAU), 269.99 nm (1.11 AU), 301.52 nm (A= 1 AU), 358.49 nm (A= 498.23 mAU); fluorescence (MeOH): λ_{exc} = 350 nm, λ_{ems} = 471.06 nm; HRMS (ESI-MS, 140 eV): *m/z* $[M+H]^+$ calculated for $C_{23}H_{19}N_2O^+$, 339.1492; found, 339.1561; RP-C18 HPLC: t_R = 15.21 min, 95. 3%.

4.1.5.5 3-ethyl-7-(1,2,3,4-tetrahydronaphthalen-6-yl)-3H-pyrrolo[3,2-f]quinolin-9(6H)-one (**23**). Compound **23** was prepared as described for compound **19** by reacting 0.302 g (0.89 mmol) of the appropriate phenylacrylate derivative **17** to yield 0.095 g of a crude product, which was purified by flash column chromatography (eluent $CHCl_3$/methanol, 9:1) to yield 0.055 g of a brown powder. Yield: 18%; R*f*: 0.65 (light blue fluorescent spot, $CHCl_3$/methanol, 9:1); mp = 228°C; ^{1}H NMR (400 MHz, $CDCl_3$) δ 1.52 - 1.46 (m, 7H, NCH_2CH_3 and H-6' e H-7'), 2.49 – 2.44 (m, 4H, H-5' e H-8'), 4.24 (q, *J* = 7.3 Hz, 2H, NCH_2CH_3), 6.59 (s, 1H, H-8), 6.83 (d, *J* = 7.7 Hz, 1H, H-1), 7.37 – 7.23 (m, 3H, H-1', H-3' and H-2), 7.59 (d, *J* = 8.5 Hz, 1H, H-4), 7.82 (d, *J* = 2.9 Hz, 1H, H-4'), 7.96 – 7.87 (d, *J* = 8.5 Hz, 1H, H-5), 11.69 (s, 1H, NH) ppm. ^{13}C NMR (101 MHz, $CDCl_3$): δ 28.47 (NCH_2CH_3), 33.94 (C-6' and C-7'), 39.01 (C-5' and C-8'), 48.74 (NCH_2CH_3), 101.98 (C-1), 106.26

(C-8) 107.99 (C-9a), 110.07 (C-4), 114.46 (C-5), 115.15 (C-9b), 117.65 (C-3'), 117.99 (C-1'), 119.32 (C-2), 120.77 (C-4'), 121.02 (C-8'a), 125.36 (C-3a), 125.82 (C-2'), 127.18 (C-4'a), 134.86 (C-5a), 158.58 (C-7), 176.24 (CO) ppm; IR (KBr): ν= 3434.28 (NH), 3089 (aliphatic C-H), 2925.98 (aliphatic C-H), 1608.75 (C=O), 1508.04 (C=C) cm^{-1}; UV-Vis (H_2O): 216.26 nm (A = 543.13 mAU), 292.38 nm (A= 660.66 mAU), 355.26 nm (252.26 mAU); fluorescence (MeOH): λ_{exc} = 350 nm, λ_{ems} = 484.02 nm; HRMS (ESI-MS, 140 eV): *m/z* $[M+H]^+$ calculated for $C_{23}H_{23}N_2O^+$, 343.1805; found, 343.1892; RP-C18 HPLC: t_R = 16.21 min, 95.36%.

4.1.5.6 7-(benzo[d][1,3]dioxol-5-yl)-3-ethyl-3H-pyrrolo[3,2-f]quinolin-9(6H)-one (**24**). Compound **24** was prepared as described for compound **19** by reacting 0.556 g (1.47 mmol) of the appropriate phenylacrylate derivative **18** to yield 0.125 g of a crude product, which was purified by flash column chromatography (eluent $CHCl_3$/methanol, 95:5) to yield 0.086 g of a brown powder. Yield: 17.6%; R*f*: 0.42 (light blue fluorescent spot, $CHCl_3$/methanol, 95:5); mp = 252°C; ^{1}H NMR (400 MHz, DMSO) δ 1.41 (t, *J* = 7.2 Hz, 3H, NCH_2CH_3), 4.32 (q, *J* = 7.2 Hz, 2H, NCH_2CH_3), 6.15 (s, 2H, OCH_2O), 6.42 (s, 1H, H-8), 7.12 (d, *J* = 8.1 Hz, 1H, H-1), 7.45 - 7.38 (m,, 2H, H-4' and H-2), 7.45 (d, *J* = 1.6 Hz, 1H, H-1'), 7.50 (m, 1H, H-4), 7.57 (d, *J* = 8.9 Hz, 1H, H-5), 7.88 (d, *J* = 9.0 Hz, 1H, H-3'), 11.27 (s, 1H, NH) ppm; ^{13}C NMR (75 MHz, $CDCl_3$): δ 20.69 (NCH_2CH_3), 40.67 (NCH_2CH_3), 95.18 (OCH_2O), 104.82 (C-1), 106.67 (C-8), 107.56 (C-4'), 108.64 (C-4), 111.72 (C-9a), 113.30 (C-5), 113.38 (C-9b), 126.11 (C-3'), 126.46 (C-1'), 126.47 (C-2), 127.91 (C-3a), 128.04 (C-2a), 128.10 (C-5a), 136.45 (C-4'b), 136.53 (C-4'a), 143.76 (C-7), 160.49 (CO) ppm; IR (KBr): ν= 3446.49 (NH), 2923.24 (aliphatic C-H), 1627.04 (C=O), 1490.04 (C=C, 1255.78 (C-O) cm^{-1}; UV-Vis (H_2O): 220.66 nm (A = 337.43 mAU), 293.52 nm (A= 305.54 mAU), 363.07 nm (206.86 mAU); fluorescence (MeOH): λ_{exc} = 350 nm, λ_{ems} = 471.96 nm; HRMS (ESI-MS, 140 eV): *m/z* $[M+H]^+$ calculated for $C_{20}H_{17}N_2O_3^+$, 333.1234; found, 333.1337; RP-C18 HPLC: t_R = 13.49 min, 98.01 %.

4.1.5.7 1-ethyl-7-phenyl-1H-pyrrolo[2,3-f]quinolin-9(6H)-one (**26**) *and 1-ethyl-7-phenyl-1H-pyrrolo[3,2-g]quinolin-5(8H)-one* (**27**). Compounds **26** and **27** were prepared as described for compound **19** by reacting 0.290 g (0.87 mmol) of the appropriate phenylacrylate derivative **25** to yield 0.186 g of a crude product consisting of the two isomers **26** and **27**. We were unable to separate the two isomers, which were characterised as a mixture. Yield: 18%; R*f*: 0.47 (light blue fluorescent spot, $CHCl_3$/methanol, 95:5); mp = 214°C; ^{1}H NMR (300 MHz, $CDCl_3$): δ 1.15 (t, J = 8.23 Hz, 3H), 1.25 (t, J = 8.23 Hz, 3H), 4.11 (q, J = 7.80 Hz, 2H), 4.12 (q, J = 7.81 Hz, 2H), 6.58 (s, 1H), 6.32 (s, 1H), 7.36 (s, 1H), 7.41 (t, J = 2.05 Hz, 1H), 7.61 (m, 2H), 7.66 (d, J = 8.66 Hz, 2H), 7.69 (m, J = 8.23 Hz, 2H), 7.72 (d, J = 3.03 Hz, 1H), 7.80 (m, J = 8.22 Hz, 2H), 7.92 (d, J = 9.46 Hz, 1H), 7.98 (m, 4H), 8.02 (d, J = 9.17 Hz, 1H), 8.14 (s, 1H), 11.67 (s, 1H, NH), 11.69 (s, 1H, NH) ppm; ^{13}C NMR (75 MHz, $CDCl_3$): δ 15.34, 15.93, 40.23, 40.34, 104.52, 105.27, 106.95, 112.24, 113.50, 118.56, 119.39, 119.65, 121.42, 121.55, 124.83, 126.29, 126.67, 126.88, 127.38, 127.59, 127.92, 128.09, 128.48, 128.99, 129.06, 129.37, 129.99, 130.43, 130.74, 131.60, 133.72, 134.02, 136.93, 137.25, 139.86, 150.67, 152.13, 179.12, 180.02 ppm. IR (KBr): ν= 3422.11 (NH), 3082.51 (aromatic C-H) 2927.42 (aliphatic C-H), 1539.89 (C=C) cm^{-1}; UV-Vis (H_2O): 219.54 nm (A = 207.13 mAU), 284.85 nm (A= 271 mAU), 296.06 nm (596.01 mAU), 359.25 nm (168.32 mAU) 377.68 (323.25 mAU); fluorescence (MeOH): λ_{exc} = 350 nm, λ_{ems} = 473.93 nm; HRMS (ESI-MS, 140 eV): *m/z* $[M+H]^+$ calculated for $C_{19}H_{17}N_2O^+$, 289.1341; found, 289.1440; RP-C18 HPLC: t_{R1} = 13.49 min, 49.52 %, t_{R2} = 19.23 min, 50.48 %.

4.1.6 1-ethyl-8-phenyl-1H-pyrrolo[3,2-h]quinolin-6(9H)-one (**29**) *and (Z)-2-phenyl-[1,4]diazepino[3,2,1-hi]indol-4(1H)-one* (**30**). Compounds **29** and **30** were prepared as described for compound **19** by reacting 1.261 g (3.77 mmol) of the appropriate phenylacrylate derivative **28** to yield 0.180 g of a crude product consisting of the two isomers **29** and **30**. The two isomers were separated by flash-column chromatography (eluent $CHCl_3$/methanol, 95:5) to yield 11 mg of

compound **29** and 0.130 g of compound **30**. Compound **29**: R*f*: 0.64 (light blue fluorescent spot, $CHCl_3$/methanol, 95:5); HRMS (ESI-MS, 140 eV): *m/z* $[M+H]^+$ calculated for $C_{19}H_{17}N_2O^+$, 289.1335; found, 289.1437; ^1H NMR (300 MHz, DMSO-d_6): δ 1.39 (t, *J* = 7.12 Hz, 3H, NCH_2CH_3), 4.27 (q, *J* = 7.11 Hz, 2H, NCH_2CH_3), 6.45 (s, 1H); 7.42 (d, J = 3.81 Hz, 1H), 7.47 (d, J= 3.21 Hz, 1H), 7.57 (d, 1H, J = 8.96 Hz), 7.65 (m, 3H), 7.89 (m, 2H), 7.97 (d, J= 8.96 Hz, 1H), 11.83 (s, 1H) ppm; ^{13}C NMR (75 MHz, DMSO-d_6): 33.24, 49.95, 101.20, 108.02, 108.74, 117.39, 117.82, 128.39, 128.98, 139.14, 139.95, 141.92, 147.02, 150.31 ppm; Compound **30**: Yield: 13.3%; R*f*: 0.79 ($CHCl_3$/methanol, 95:5); ^1H NMR (300 MHz, DMSO-d_6): δ 6.75 (s, 1H, H-3), 7.13 (m, 3H, 3′-, 4’- and 5′-H), 7.25 (d, J = 2.73 Hz, 1H, H-6), 7.50 (d, J = 2.73 Hz, 1H, H-5), 7.75 (d, 1H, J = 9.00 Hz, 1H, H-7), 7.85 (m, 1H, H-8), 8.10 (d, J = 9.00 Hz, 1H, H-9), 8.33 (m, 2H, 2′- and 6′-H), 11.81 (s, 1H, NH) ppm; ^{13}C NMR (75 MHz, DMSO-d_6): δ 98.03 (C-3), 102.12 (C-6), 125.87 (C-5), 128.58 (C-4'), 128.85 (C-2' e C-6’), 129.30 (C-3' e C-5’), 130.51 (C-6a), 131.74 (C-7), 133.28 (C-8), 133.77 (C-9), 137.25 (C-1'), 160.73 (C-9a), 161.31 (C-2), 170.38 (C-4), 192.87 (C-9b) ppm; IR (KBr): ν= 3447.85 (NH), 3098.88 (aromatic C-H), 1740.47 (C=ONR1R2 stretching), 1626.09 (C=ONR1R2 stretching), 1548.79 cm-1 (C=C); UV-Vis (H_2O): 222.36 nm (A= 635.15 mAU), 357.76 nm (A= 894.41 mAU); ESI-MS: *m/z* $[M+H]^+$ calculated for $C_{17}H_{13}N_2O^+$, 261.1022, found 293.0904 $(M+H+CH_3OH]^+$; RP-C18 HPLC: t_{R1} = 18.03 min, 95.01%.

4.2 Biological assays

4.2.1 Cell growth conditions and antiproliferative assay

Human T-cell leukemia (Jurkat and CEM), human B-cell leukemia (RS4;11) and human myeloid leukemia (Kasumi-1) cells were grown in RPMI-1640 medium (Gibco, Milano, Italy). Breast adenocarcinoma (MDA-MB-231), human cervix carcinoma (HeLa), non-small cell lung adenocarcinoma (A549) and human colon adenocarcinoma (HT-29) cells were grown in DMEM medium (Gibco, Milano, Italy), all supplemented with 115 units/mL penicillin G (Gibco, Milano,

Italy), 115 μg/mL streptomycin (Invitrogen, Milano, Italy), and 10% fetal bovine serum (Invitrogen, Milano, Italy). Stock solutions (10 mM) of the different compounds were obtained by dissolving them in DMSO. Individual wells of a 96-well tissue culture microtiter plate were inoculated with 100 μL of complete medium containing 8×10^3 cells. The plates were incubated at 37 °C in a humidified 5% CO_2 incubator for 18 h prior to the experiments. After medium removal, a 100 μL aliquot of fresh medium containing the test compound at a varying concentration was added to each well in triplicate and incubated at 37 °C for 72 h. Cell viability was assayed by the (3-(4, 5-dimethylthiazol-2-yl)-2,5-diphenyltetrazolium bromide test as previously described [22]. The GI_{50} was defined as the compound concentration required to inhibit cell proliferation by 50%.

$CEM^{Vbl-100}$ cells are a multidrug-resistant line selected against vinblastine and were a kind gift of Dr. G. Arancia (Istituto Superiore di Sanità, Rome, Italy). They were grown in RPMI-1640 medium supplemented with 100 ng/mL of vinblastine.

Peripheral blood lymphocytes (PBL) from healthy donors were obtained by separation on a Lymphoprep (Fresenius KABI Norge AS) gradient. After extensive washing, cells were resuspended (1.0×10^6 cells/mL) in RPMI-1640 with 10% fetal bovine serum and incubated overnight. For cytotoxicity evaluations in proliferating PBL cultures, non-adherent cells were resuspended at 5×10^5 cells/mL in growth medium containing 2.5 μg/mL PHA (Irvine Scientific). Different concentrations of the test compounds were added, and viability was determined 72 h later by the MTT test. For cytotoxicity evaluations in resting PBL cultures, non-adherent cells were resuspended (5×10^5 cells/mL) and treated for 72 h with the test compounds, as described above.

4.2.2 Effects on tubulin polymerization and on colchicine binding to tubulin

To evaluate the effect of the compounds on tubulin assembly *in vitro* [12], varying concentrations of compounds were preincubated with 10 μM bovine brain tubulin in 0.8 M monosodium glutamate (from a 2 M stock solution adjusted to pH 6.6 with HCl) for 15 min at 30 ˚C and then cooled to 0 ˚C. After addition of 0.4 mM GTP (final concentration), the mixtures were transferred to 0 °C cuvettes in a recording spectrophotometer equipped with an electronic temperature controller and warmed to 30 °C. Tubulin assembly was followed turbidimetrically at 350 nm. The IC_{50} was defined as the compound concentration that inhibited the extent of assembly by 50% after a 20 min incubation. The ability of the test compounds to inhibit colchicine binding to tubulin was measured as described [13], with the reaction mixtures containing 1 μM tubulin, 5 μM [^{3}H]colchicine and 1 or 5 μM test compound.

4.2.3 Molecular modeling

Compounds in Table 1 were built and their partial charges calculated after semi-empirical (PM6) energy minimization using MOE2016 [32,33]. The molecular docking studies were based on the protocol recently reported for this target [8]. Briefly, the more suitable docking protocol was identified using a benchmark over 14 protein/scoring protocol using DockBench 1.01[34], a tool that compared the performance of 14 different posing/scoring protocols. Each ligand was docked 20 times using GOLD using PLP [35], the virtual screening tool of DockBench adopting the parameters already used in the benchmark study. The SARs of compounds **26**-**27** were not investigated by molecular docking because biological data was not available for these compounds.

To facilitate the visualization and analysis of data obtained from the docking simulations, we produced a video that shows the most relevant docking data, such as docking poses, per residue IEhyd and IEele data, experimental binding data and scoring values. Details for the video

production were recently reported [9]. The logP values were predicted by the Stardrop software package [36].

4.2.4 Flow cytometric analysis of cell cycle distribution

5×10^5 HeLa cells were treated with different concentrations of the test compounds for 24 h. After the incubation period, the cells were collected, centrifuged, and fixed with ice-cold ethanol (70%). The cells were then treated with lysis buffer containing RNase A and 0.1% Triton X-100 and stained with PI. Samples were analyzed on a Cytomic FC500 flow cytometer (Beckman Coulter). DNA histograms were analyzed using MultiCycle for Windows (Phoenix Flow Systems).

4.2.5 Apoptosis assay

Cell death was determined by flow cytometry of cells double stained with annexin V/FITC and PI. The Coulter Cytomics FC500 (Beckman Coulter) was used to measure the surface exposure of PS on apoptotic cells according to the manufacturer's instructions (Annexin-V Fluos, Roche Diagnostics).

4.2.6 Analysis of mitochondrial potential and ROS

The mitochondrial membrane potential was measured with the lipophilic cation JC-1 (Molecular Probes, Eugene, OR, USA), while the production of ROS was followed by flow cytometry using the fluorescent dyes H_2DCFDA (Molecular Probes), as previously described [23].

4.2.7 Western blot analysis

HeLa cells were incubated in the presence of **23** and, after different times, were collected, centrifuged, and washed two times with ice cold phosphate buffered saline (PBS). The pellet was then resuspended in lysis buffer. After the cells were lysed on ice for 30 min, lysates were centrifuged at 15000 x g at 4 °C for 10 min. The protein concentration in the supernatant was determined using the BCA protein assay reagents (Pierce, Italy). Equal amounts of protein (10 μg) were resolved using sodium dodecyl sulfate-polyacrylamide gel electrophoresis (SDS-PAGE) (Criterion Precast, BioRad, Italy) and transferred to a PVDF Hybond-P membrane (GE Healthcare). Membranes were blocked with a bovine serum albumin solution (5% in Tween PBS 1X), and the membranes being gently rotated overnight at 4 °C. Membranes were then incubated with primary antibodies against Bcl-2, PARP, cdc25c, cyclin B, p-cdc2^{Tyr15}, Mcl-1 (all from Cell Signaling) and γ-tubulin (Sigma-Aldrich) for 2 h at room temperature. Membranes were next incubated with peroxidase labeled secondary antibodies for 60 min. All membranes were visualized using ECL Select (GE Healthcare), and images were acquired using an Uvitec-Alliance imaging system (Uvitec, Cambridge, UK). To ensure equal protein loading, each membrane was stripped and reprobed with anti-γ-tubulin antibody.

Acknowledgment

The computational work coordinated by S.M., as well as synthesis by M.G. Ferlin and biological evaluation by G. Viola, were supported with financial support from the University of Padova, Italy. The work of M.S. was supported by the University of Padova, Italy (UNIPD, Progetto Giovani Studiosi 2013: Protocol number 79122). Molecular Modeling Section lab is also very grateful to the Chemical Computing Group for its scientific and technical partnership. S.M. participates in the European COST Action CM1207 (GLISTEN).

Disclaimer

The content of this paper is solely the responsibility of the authors and does not necessarily reflect the official views of the National Institutes of Health.

References

[1] C. Dumontet, M.A. Jordan, Microtubule-binding agents: a dynamic field of cancer therapeutics, Nat. Rev. Drug Discov. 9 (2010) 790–803. doi:10.1038/nrd3253.

[2] Y. Lu, J. Chen, M. Xiao, W. Li, D.D. Miller, An overview of tubulin inhibitors that interact with the colchicine binding site, Pharm. Res. 29 (2012) 2943–2971. doi:10.1007/s11095-012-0828-z.

[3] V. Gasparotto, I. Castagliuolo, G. Chiarelotto, V. Pezzi, D. Montanaro, P. Brun, G. Palù, G. Viola, M.G. Ferlin, Synthesis and biological activity of 7-phenyl-6,9-dihydro-3*H*-pyrrolo[3,2-*f*]quinolin-9-ones: a new class of antimitotic agents devoid of aromatase activity, J. Med. Chem. 49 (2006) 1910–5. doi:10.1021/jm070534b.

[4] V. Gasparotto, I. Castagliuolo, M.G. Ferlin, 3-Substituted 7-phenyl-pyrroloquinolinones show potent cytotoxic activity in human cancer cell lines, J. Med. Chem. 50 (2007) 5509–5513. doi:10.1002/cmdc.201000180.

[5] M.G. Ferlin, R. Bortolozzi, P. Brun, I. Castagliuolo, E. Hamel, G. Basso, G. Viola, Synthesis and in vitro evaluation of 3*H*-pyrrolo[3,2-*f*]-quinolin-9-one derivatives that show potent and selective anti-leukemic activity, ChemMedChem. 5 (2010) 1373–1385. doi:10.1002/cmdc.201000180.

[6] G. Viola, R. Bortolozzi, E. Hamel, S. Moro, P. Brun, I. Castagliuolo, M.G. Ferlin, G. Basso, MG-2477, a new tubulin inhibitor, induces autophagy through inhibition of the Akt/mTOR pathway and delayed apoptosis in A549 cells, Biochem. Pharmacol. 83 (2012) 16–26. doi:10.1016/j.bcp.2011.09.017.

[7] D. Carta, M.G. Ferlin, An overview on 2-arylquinolin-4(1*H*)-ones and related structures as

tubulin polymerisation inhibitors, Curr. Top. Med. Chem. 2322 (2014) 2322–2345.

[8] D. Carta, R. Bortolozzi, E. Hamel, G. Basso, S. Moro, G. Viola, M.G. Ferlin, Novel 3-substituted 7-phenylpyrrolo[3,2-*f*]quinolin-9(6*H*)-ones as single entities with multitarget Antiproliferative Activity, J. Med. Chem. 58 (2015) 7991–8010. doi:10.1021/acs.jmedchem.5b00805.

[9] D. Carta, R. Bortolozzi, M. Sturlese, V. Salmaso, E. Hamel, G. Basso, L. Calderan, L. Quintieri, S. Moro, G. Viola, M.G. Ferlin, Synthesis, structure-activity relationships and biological evaluation of 7-phenyl-pyrroloquinolinone 3-amide derivatives as potent antimitotic agents, Eur. J. Med. Chem. 127 (2017) 643–660. doi:10.1016/j.ejmech.2016.10.026.

[10] J. Nakano, N. Katagiri, T. Kato, Studies on ketene and its derivatives. CX. Synthesis of 1,3-dimethoxyfluoren-9-ones, Chem. Pharm. Bull. (Tokyo). 30 (1982) 2590–2594. doi:10.1248/cpb.30.2590.

[11] R. Romagnoli, P.G. Baraldi, M.K. Salvador, F. Prencipe, V. Bertolasi, M. Cancellieri, A. Brancale, E. Hamel, I. Castagliuolo, F. Consolaro, E. Porcù, G. Basso, G. Viola, Synthesis, antimitotic and antivascular activity of 1-(3',4', 5'-trimethoxybenzoyl)-3-arylamino-5-amino-1,2,4-triazoles, J. Med. Chem. 57 (2014) 6795–6808. doi:10.1021/jm5008193.

[12] E. Hamel, Evaluation of antimitotic agents by quantitative comparisons of their effects on the polymerization of purified tubulin, Cell Biochem. Biophys. 38 (2003) 1–22. doi:10.1385/CBB:38:1:1.

[13] P. Verdier-Pinard, J.Y. Lai, H.D. Yoo, J. Yu, B. Marquez, D.G. Nagle, M. Nambu, J.D. White, J.R. Falck, W.H. Gerwick, B.W. Day, E. Hamel, Structure-activity analysis of the interaction of curacin A, the potent colchicine site antimitotic agent, with tubulin and effects of analogs on the growth of MCF-7 breast cancer cells, Mol. Pharmacol. 53 (1998) 62–76. doi:10.1124/mol.53.1.62.

[14] B.A.A. Weaver, D.W. Cleveland, Decoding the links between mitosis, cancer, and chemotherapy: The mitotic checkpoint, adaptation, and cell death, Cancer Cell 8 (2005) 7–12. doi:10.1016/j.ccr.2005.06.011.

[15] P.R. Clarke, L.A. Allan, Cell-cycle control in the face of damage - a matter of life or death, Trends Cell Biol. 19 (2009) 89–98. doi:10.1016/j.tcb.2008.12.003.

[16] I. Vitale, A. Antoccia, C. Cenciarelli, P. Crateri, S. Meschini, G. Arancia, C. Pisano, C. Tanzarella Combretastatin CA-4 and combretastatin derivative induce mitotic catastrophe dependent on spindle checkpoint and caspase-3 activation in non-small cell lung cancer cells. Apoptosis. 12 (2007) 155-66.

[17] C. Cenciarelli, C.Tanzarella, I. Vitale, C. Pisano, P. Crateri, S. Meschini, G. Arancia, A. Antoccia The tubulin-depolymerising agent combretastatin-4 induces ectopic aster assembly and mitotic catastrophe in lung cancer cells H460. Apoptosis. 13 (2008) 659-69. doi: 10.1007/s10495-008-0200-2.

[18] Y. Tsujimoto, S. Shimizu, Role of the mitochondrial membrane permeability transition in cell death, Apoptosis 12 (2007) 835–840. doi:10.1007/s10495-006-0525-7.

[19] S. Xiong, T. Mu, G. Wang, X. Jiang, Mitochondria-mediated apoptosis in mammals, Protein Cell 5 (2014) 737–749. doi:10.1007/s13238-014-0089-1.

[20] E. Lugli, L. Troiano, A. Cossarizza, Polychromatic analysis of mitochondrial membrane potential using JC-1, Curr. Protoc. Cytom. Chapter 7 (2007) Unit 7.32. doi:10.1002/0471142956.cy0732s41.

[21] A. Rovini, A. Savry, D. Braguer, M. Carré, Microtubule-targeted agents: When mitochondria become essential to chemotherapy, Biochim. Biophys. Acta - Bioenerg. 1807 (2011) 679–688. doi:10.1016/j.bbabio.2011.01.001.

[22] R. Romagnoli, P.G. Baraldi, C. Lopez-Cara, D. Preti, M. Aghazadeh Tabrizi, J. Balzarini, M. Bassetto, A. Brancale, X.H. Fu, Y. Gao, J. Li, S.Z. Zhang, E. Hamel, R. Bortolozzi, G. Basso, G. Viola, Concise synthesis and biological evaluation of 2-Aroyl-5-

Amino benzo[*b*]thiophene Derivatives As a Novel Class of Potent Antimitotic Agents, J. Med. Chem. 56 (2013) 9296–9309. doi:10.1021/jm4013938.

[23] R. Romagnoli, P.G. Baraldi, M.K. Salvador, F. Prencipe, C. Lopez-Cara, S. Schiaffino Ortega, A. Brancale, E. Hamel, I. Castagliuolo, S. Mitola, R. Ronca, R. Bortolozzi, E. Porcuì, G. Basso, G. Viola, Design, synthesis, in vitro, and in vivo Anticancer and Antiangiogenic Activity of Novel 3-Arylaminobenzofuran Derivatives Targeting the Colchicine Site on Tubulin, J. Med. Chem. 58 (2015) 3209–3222. doi:10.1021/acs.jmedchem.5b00155.

[24] N. Zamzami, P. Marchetti, M. Castedo, D. Decaudin, A. Macho, T. Hirsch, S.A. Susin, P.X. Petit, B. Mignotte, G. Kroemer, Sequential reduction of mitochondrial transmembrane potential and generation of reactive oxygen species in early programmed cell death, J. Exp. Med. 182 (1995) 367–77. doi:10.1084/jem.182.2.367.

[25] Cai, D.P. Jones, Superoxide in apoptosis. Mitochondrial generation triggered by cytochrome c loss, J. Biol. Chem. 273 (1998) 11401–11404.

[26] Nohl, L. Gille, K. Staniek, Intracellular generation of reactive oxygen species by mitochondria, Biochem. Pharmacol. 69 (2005) 719–723. doi:10.1016/j.bcp.2004.12.002.

[27] G. Rothe, G. Valet, Flow cytometric analysis of respiratory burst activity in phagocytes with hydroethidine and 2',7'-dichlorofluorescin, J. Leukoc. Biol. 47 (1990) 440–448.

[28] Harley, L.A. Allan, H.S. Sanderson, P.R. Clarke, Phosphorylation of Mcl-1 by cdk1-cyclin B1 initiates its cdc20-dependent destruction during mitotic arrest, EMBO J. 29 (2010) 2407–2420. doi:10.1038/emboj.2010.112.

[29] I.E. Wertz, S. Kusam, C. Lam, T. Okamoto, W. Sandoval, D.J. Anderson, E. Helgason, J.A. Ernst, M. Eby, J. Liu, L.D. Belmont, J.S. Kaminker, K.M. O'Rourke, K. Pujara, P.B. Kohli, A.R. Johnson, M.L. Chiu, J.R. Lill, P.K. Jackson, W.J. Fairbrother, S. Seshagiri, M.J.C. Ludlam, K.G. Leong, E.C. Dueber, H. Maecker, D.C.S. Huang, V.M.

Dixit, Sensitivity to antitubulin chemotherapeutics is regulated by MCL1 and FBW7, Nature. 471 (2011) 110–114. doi:10.1038/nature09779.

[30] D. Haschka, C. Soratroi, S. Kirschnek, G. Häcker, R. Hilbe, S. Geley, A. Villunger, L.L. Fava, The NOXA–MCL1–BIM axis defines lifespan on extended mitotic arrest, Nat. Commun. 6 (2015) 6891. doi:10.1038/ncomms7891.

[31] Y. Wang, H. Zhang, B. Gigant, Y. Yu, Y. Wu, X. Chen, Q. Lai, Z. Yang, Q. Chen, J. Yang, Structures of a diverse set of colchicine binding site inhibitors in complex with tubulin provide a rationale for drug discovery, FEBS J. 283 (2016) 102–111. doi:10.1111/febs.13555.

[32] J.J.P. Stewart, Optimization of parameters for semiempirical methods V: Modification of NDDO approximations and application to 70 elements, J. Mol. Model. 13 (2007) 1173–1213. doi:10.1007/s00894-007-0233-4.

[33] Chemical Computing Group (CCG) Inc. Molecular Operating Environment (MOE); Chemical Computing Group: 1010 Sherbooke St. West, Suite #910, Montreal, QC, Canada, H3A 2R7, 2016

[34] A.Cuzzolin; M.Sturlese; I. Malvacio; A. Ciancetta; S. Moro. Molecules. DockBench: An Integrated Informatic Platform Bridging the Gap between the Robust Validation of Docking Protocols and Virtual Screening Simulations.20 (2015), 9977–9993

[35] GOLD suite, version 5.2 (Internet). Cambridge Crystallographic Data Centre: 12 Union Road, Cambridge CB2 1EZ, UK. Available from: http://www.ccdc.cam.ac.uk

[36] StarDrop. Optibrium Ltd, 7221 Cambridge Research Park, Beach Drive, Cambridge, CB25 9TL, UK. http://www.optibrium.com/.

Table 1: In vitro cell growth inhibitory effects of compounds **19-24, 26-27** and **29-31**

compound	GI_{50} (nM) [a]						
	HeLa	A549	HT-29	MDA-MB-231	RS4;11	Jurkat	Kasumi-1
19	2380±400	3400±400	>10000	>10000	>10000	>10000	>10000
20	8350±440	820±140	>10000	5362±2043	>10000	>10000	>10000
21	0.5±0.03	4.2±0.7	1.9±0.7	17.1±9.4	0.5±0.05	0.7±0.002	0.4±0.1
22	714±2.9	744±26	376±58	465±43	22±2	32±4	396±39
23	34±0.35	45±0.94	4.7±0.5	591±35	7±0.8	3±0.02	15±2
24	4.2±0.3	1.1± 0.3	0.6±0.04	123±8.8	0.2±0.05	0.1±0.002	0.3±0.09
26-27	49±0.16	7.1±0.75	16.0±3.3	641±57	13±1.5	27±2	30±2
29	5920±186	9590±9.9	>10000	>10000	>10000	>10000	>10000
30	>10000	>10000	>10000	>10000	>10000	>10000	>10000
31[b]	11±8	32±1.5	32±1.2	n.d.	2±0.3	0.5±0.2	n.d
CA-4[c]	4.0±1.0	180±50	3100±100	n.d.	0.8±0.2	5.0±0.6	n.d.

[a] IC_{50}= compound concentration required to inhibit tumor cell proliferation by 50%. Data are expressed as the mean ± SE from the dose-response curves of at least three independent experiments. n.d. not determined

[b] Data taken from Ref. 4 and 8

[c] Data taken from Ref. 8 and 20

Table 2. Cytotoxicity of compounds **21** and **24** for human peripheral blood lymphocytes (PBL)

	GI_{50} (μM)[a]	
	21	**24**
$PBL_{resting}$[b]	>100	45.3±1.4
PBL_{PHA}[c]	25.7±1.2	23.0±1.5

[a]Compound concentration required to reduce cell growth by 50%.

[b] $PBL_{resting}$ not stimulated with PHA.

[c] PBL_{PHA} stimulated with PHA.

Values are the mean ± SEM from three separate experiments.

Table 3. Cytotoxicity of **21** and **24** in multidrug resistant cells

	IC_{50} (nM) [a]	
	CEM^{wt}	CEM^{Vbl100}
21	29.8±1.4	2.3±0.4
24	27.8±0.81	3.7±0.9
Vinblastine	1.5 ± 0.3	285 ± 69

[a]Compound concentration required to reduce cell growth inhibition by 50%.

Values are the mean ± SEM for three separate experiments.

Table 4. Inhibition of tubulin polymerization and colchicine binding by compounds **21, 23, 24** and **26-27**

Compound	Inhibition of tubulin assembly IC_{50} (μM) ± SD[a]	Inhibition of colchicine binding % Inhibition ± SD[b]
21	0.99±0.07	46±2
23	1.1±0.1	26±0.6
24	0.84± 0.05	49±2
26-27	6.2±0.5	24±4
31[c]	0.57±0.02	73±0.7
CA-4	0.64±0.01	98±0.1

[a] Inhibition of tubulin polymerization. Tubulin was at 10 μM.

[b] Inhibition of [^{3}H]colchicine binding. Tubulin and colchicine were at 1 and 5 μM, respectively.

[c.] Data taken from Ref. 4

Figure legends

Figure 1.

Structure-activity relationships of 7-pyrrolo[3,2-*f*]quinolinones. The three main structural determinants for potent cytotoxicity modified for obtaining novel PyQs were the 3- and 7-substituents and the angular geometry

Figure 2

Percentage of cells in each phase of the cell cycle in HeLa cells treated with compounds **21** (A), **23** (B) and **24** (C) at the indicated concentrations for 24 h. Cells were fixed and labeled with PI and analyzed by flow cytometry as described in the Experimental Section. Data are presented as mean of two independent experiments ± SEM.

Figure 3

Effect of compound **24** on cell cycle checkpoint proteins. HeLa cells were treated for 24 or 48 h with the indicated concentrations of **24**. The cells were harvested and lysed for detection of the expression of the indicated protein by western blot analysis. To confirm equal protein loading, each membrane was stripped and reprobed with anti-γ-tubulin antibody.

Figure 4

Flow cytometric analysis of apoptotic cells after treatment of A549 (Panels A and B) and HeLa cells (Panel C and D) with **21, 23** or **24** at the indicated concentrations after incubation for 24 (A,C) or 48 h (B,D). The induction of apoptosis was also evaluated in Hela cells (panel E) with CA-4 (0.1 μM) chosen as reference compound. The cells were harvested and labeled with annexin-V-FITC and PI and analyzed by flow cytometry. Data are presented as mean±SEM of three independent experiments.

Figure 5

Panel A. Assessment of mitochondrial membrane potential ($\Delta\psi_{mt}$) after treatment of HeLa cells with compound **24**. Cells were treated with the indicated concentration of compound for 6, 12, 24 or 48 h and then stained with the fluorescent probe JC-1 for analysis of mitochondrial potential. Cells were then analyzed by flow cytometry as described in the Experimental Section. Data are presented as mean±SEM of three independent experiments. Panel B. Assessment of ROS production after treatment of HeLa cells with compound **24**. Cells were treated with the indicated concentration of compound for 6 , 12, 24 or 48 h and then stained with H_2-DCFDA for the evaluation of ROS levels. Cells were then analyzed by flow cytometry as described in the Experimental Section. Data are presented as mean±SEM of three independent experiments.

Figure 6. Western blot analysis of Bcl-2, Mcl-1 and PARP after treatment of HeLa cells with **24** at the indicated concentrations and for the indicated times. To confirm equal protein loading, each membrane was stripped and reprobed with anti-γ-tubulin antibody.

Figure 7. The energetically most favorable pose of compound **21**-**24** (magenta) obtained by molecular docking simulation using the protein conformation of the plinabulin complex (PDB ID: 5C8Y). The ribbon, as well as the residue atoms of the colchicine site, are colored according to the subunit to which they belong: white for β-tubulin and orange for α-tubulin. Hydrogen atoms are not shown. Hydrogen bonds are indicated in red.

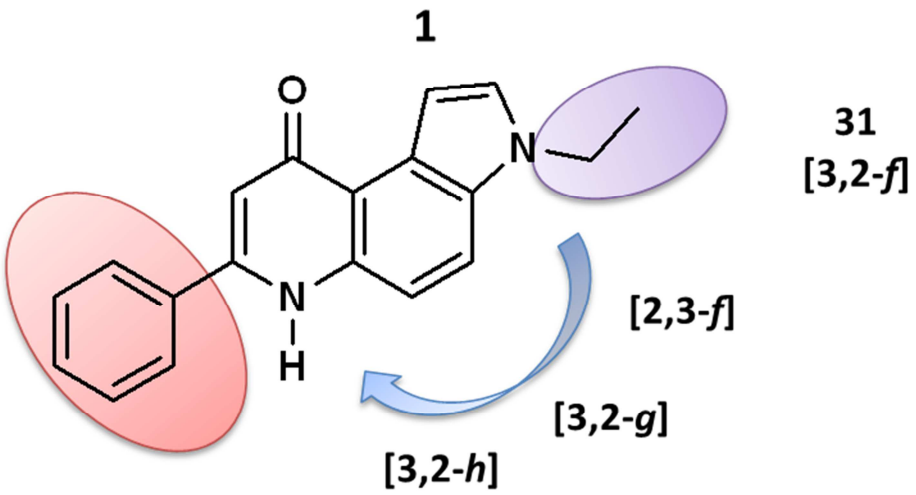

Figure 1

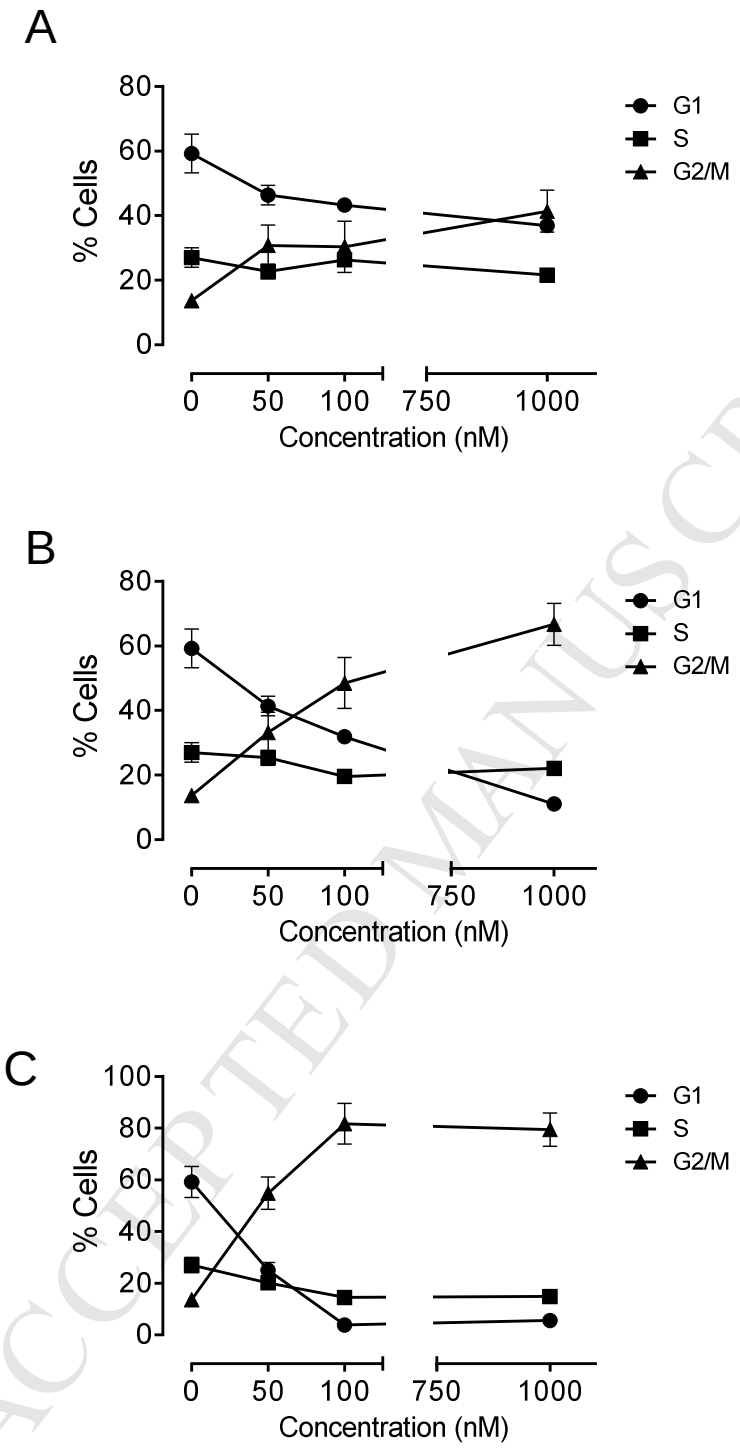

Figure 2

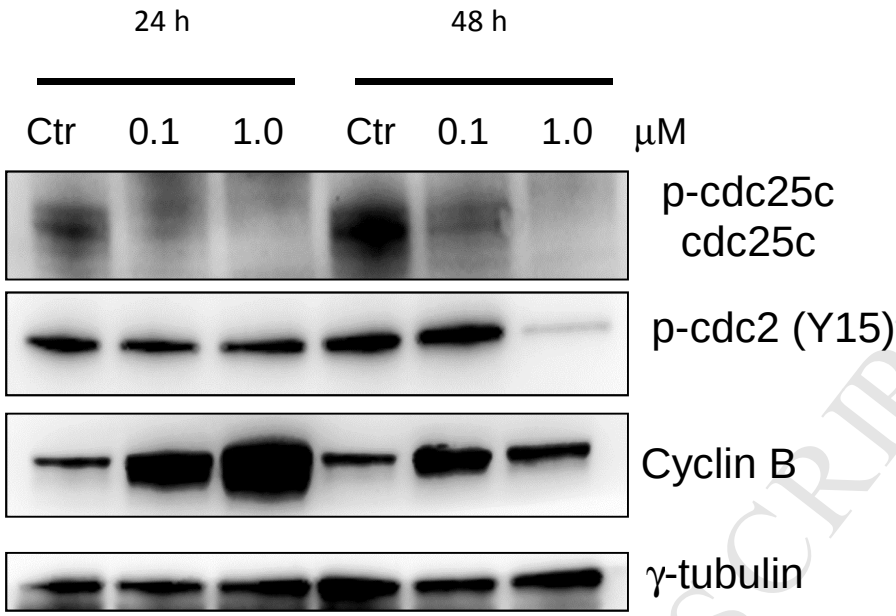

Figure 3

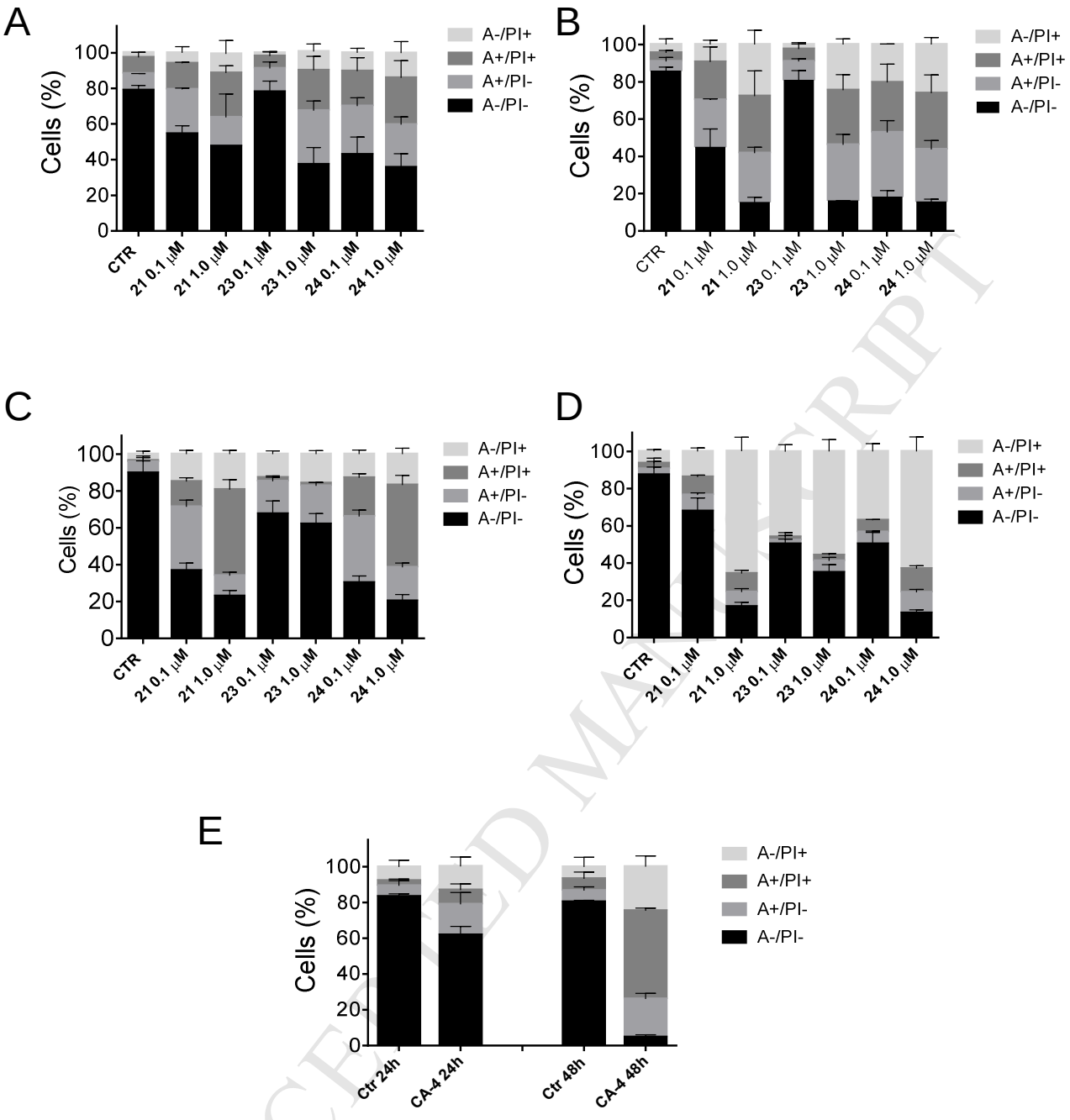

Figure 4

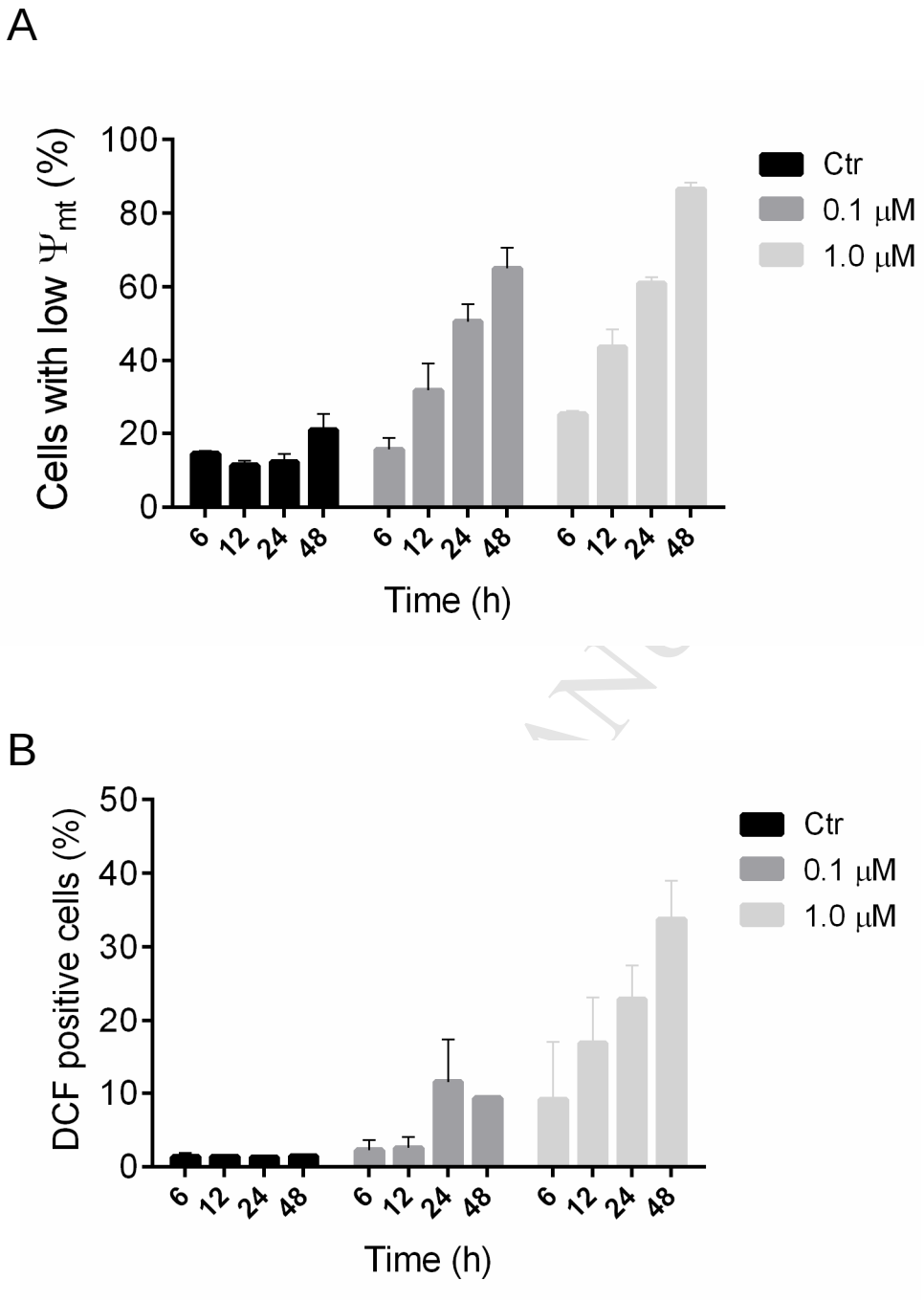
A
Cells with low Ψmt (%)
100
80
60
40
20
0
6 12 24 48 6 12 24 48 6 12 24 48
Time (h)
Ctr
0.1 μM
1.0 μM
B
DCF positive cells (%)
50
40
30
20
10
0
6 12 24 48 6 12 24 48 6 12 24 48
Time (h)
Ctr
0.1 μM
1.0 μM

Figure 5

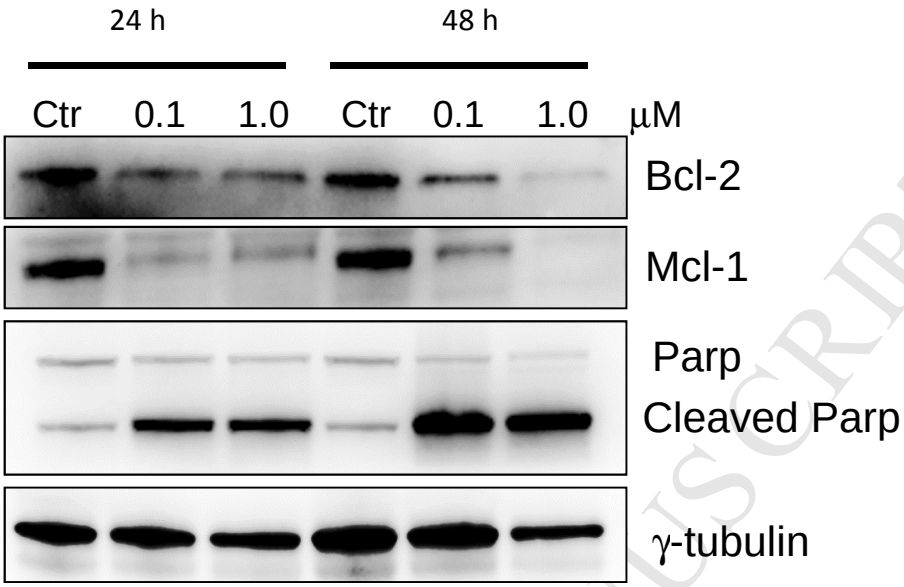

Figure 6

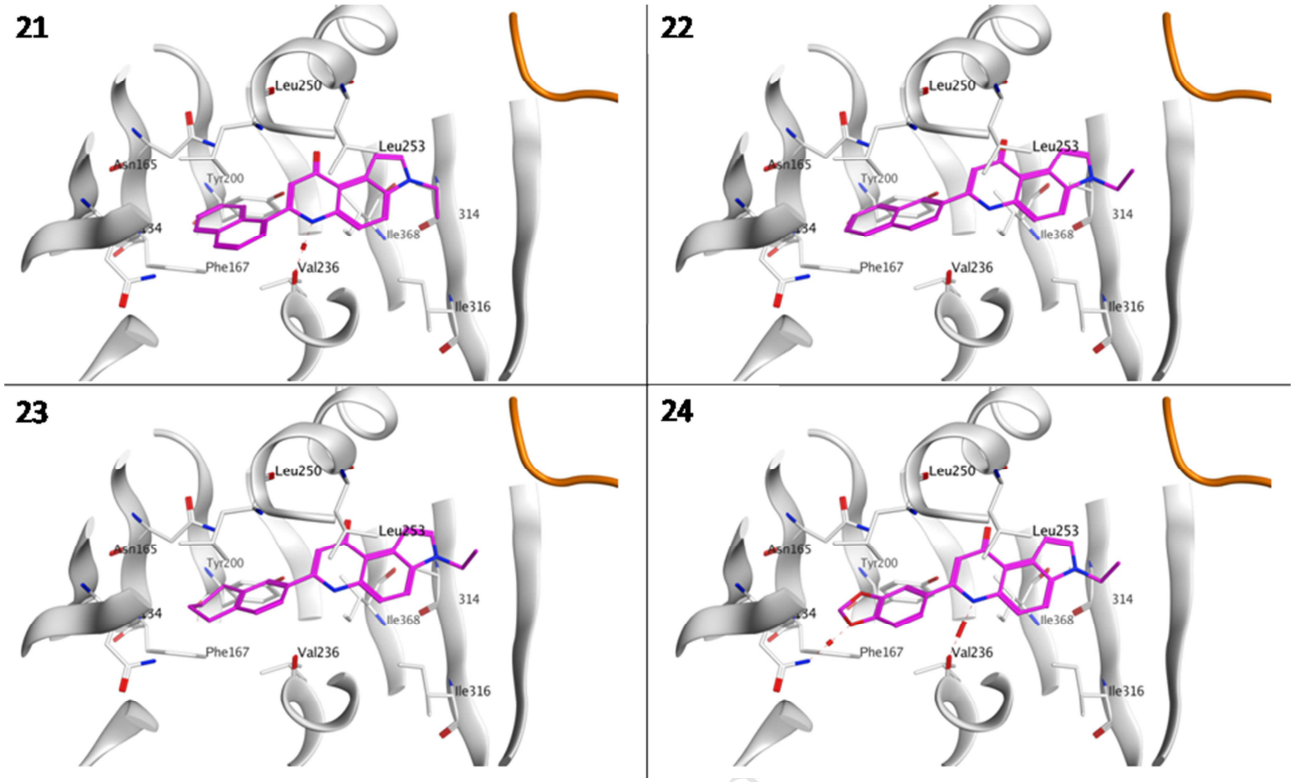

Figure 7

Scheme 1: a) NaH, NaI, bromoethane or *n*-octadecyl-Cl, DMF, 50 °C, 6 h; b) H_2, Pd/C 10%, EtOAc, 55 °C, 12 h; c) NaH 60%, anhydrous dioxane, 80 °C, 6 h; d) abs EtOH, AcOH, drierite, 100 °C, 48 h; e) Ph_2O, 250 °C, 15 min.

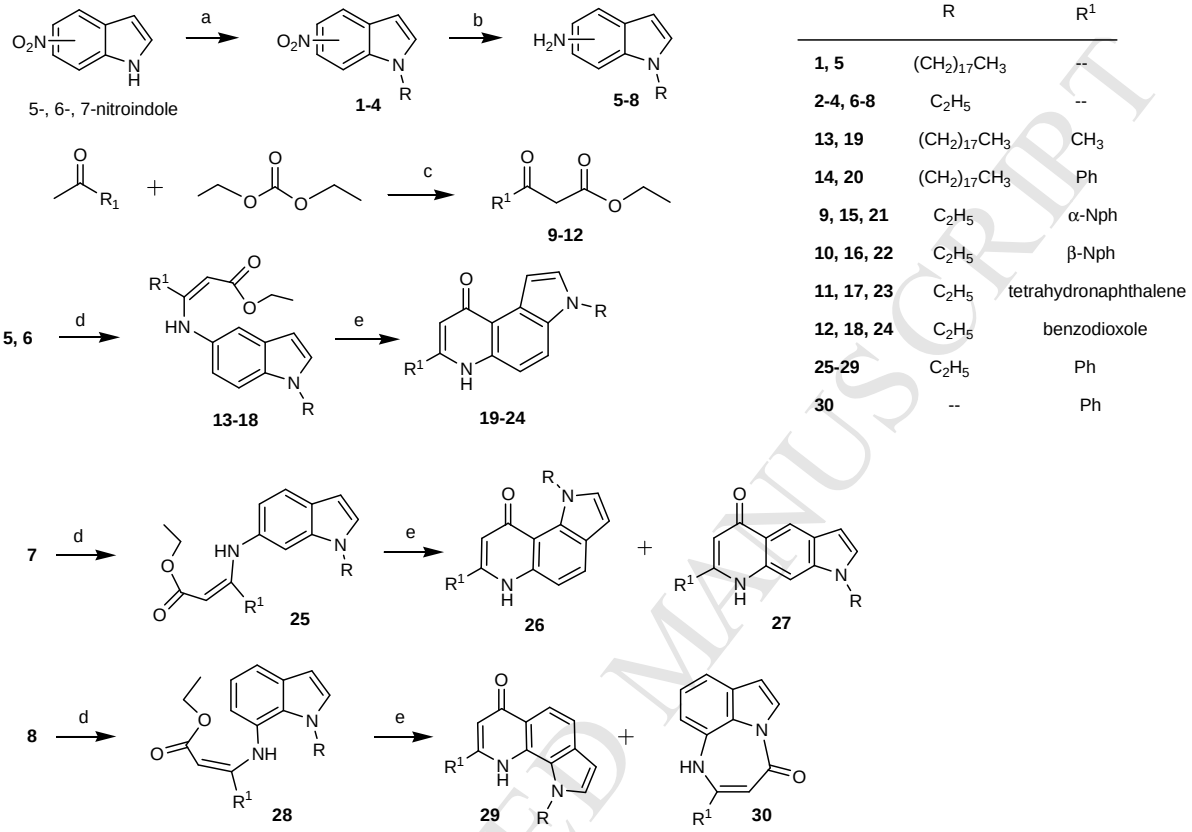

	R	R^1
1, 5	$(CH_2)_{17}CH_3$	--
2-4, 6-8	C_2H_5	--
13, 19	$(CH_2)_{17}CH_3$	CH_3
14, 20	$(CH_2)_{17}CH_3$	Ph
9, 15, 21	C_2H_5	α-Nph
10, 16, 22	C_2H_5	β-Nph
11, 17, 23	C_2H_5	tetrahydronaphthalene
12, 18, 24	C_2H_5	benzodioxole
25-29	C_2H_5	Ph
30	--	Ph

Highlights

- A small library of 7-pyrrolo[3,2-*f*]quinolinones was synthesized
- One of the most active compound **24** showed GI_{50}s ranging from 0.2 to 123 nM
- Compound **24** did not induce significant cell death in normal human lymphocytes
- Compound **24** overcomes multi-drug resistance
- Compounds, **24** strongly inhibited tubulin assembly assay with an IC_{50} of 0.84 μM
- Compound **24** induce apoptosis through the mitochondrial pathway